Tuning of the reflection and spontaneous emission of a one-dimensional photonic crystal

by

Elizabeth Galindo Linares

A dissertation submitted to the program in Electronics, in partial
fulfillment of the requirements for the degree of

**MASTER OF SCIENCES IN
ELECTRONICS**

at the

**National Institute of Astrophysics, Optics and
Electronics**

January 2007

Tonantzintla, Puebla

Supervised by:

Dr. Peter Peretz Halevi Sar, INAOE

Abstract

In this thesis I consider tuning of the optical response of a one-dimensional photonic crystal. The optical response is represented by (a) reflectance and (b) spontaneous emission. In both cases the photonic crystal is constituted from alternating silicon (Si) and silica (SiO_2) layers. The density of free carriers in the Si layers is modulated at a level of $10^{19}/\mathrm{cm}^3$, the wavelength of light being fixed at 1.54μm.

(a) I calculate the tuning of reflectance of a one-dimensional photonic crystal (PC) by means of charge injection. The PC is constituted from highly doped Si layers alternating with SiO_2 layers. The wavelength of the light is assumed to be the important communications wavelength of $1.54\mu m$. A realistic calculation shows that sensitive tuning, and switching as well, can be achieved for an impurity density $\sim 10^{19}/cm^3$ even for superlattices (SLs) only a few periods long. The reflectance results are satisfactorily interpreted in terms of photonic band (PB) structure calculations.

(b) If the modal density available to an excited atom is varied on the time scale of its lifetime, then we can expect the natural process of spontaneous emission (SE) to become dynamically manipulable. I consider various experimental possibilities and focus on an atom embedded in a PC designed to have a band edge in the vicinity of the frequency of the emitted light. Specifically, I calculate the rate of SE by erbium ions (radiating at the wavelength $1.54\mu m$) implanted in a one-dimensional Si/SiO_2 PC. The semiconductor layers are assumed to be strongly doped; by tuning the impurity density the free carrier concentration changes and the PBs shift. As a result, the SE rate exhibits significant dependency on the level of charge injection. The body of the thesis consists of two papers, corresponding to (a) and (b) above.

One of these has been already accepted for publication, while the other has been submitted for publication. Their preprints are enclosed at the end of the thesis.

Aknowledgments

Dr. Peter Halevi and Dr. Adán Sánchez por compartirme sus conocimientos, enseñzas y paciencia.

Al Consejo Nacional de Ciencia y Tecnología (CONACyT) y al Sistema Nacional de Investigadores (SNI)por el apoyo económico dado, sin el cual hubiera sido imposible la realización de mis estudios y la ampliación del proyecto de investigación.

Al Dr. José Soto Eguibar, Carmen, Marina, Edith, Martha Olmos y Rocío Rodas por su comprensión y apoyo en toda dificultad y papeleo.

A mis amigos y compañeros por la ayuda, bondad, amor y sobre todo el valioso tiempo que me dedicaron. El mejor regalo fue su tiempo y las enseñanzas que me dejan son incalculables, sobre todo gracias por enseñarme a ser un mejor ser humano.

A los sinodales: Dr. Adán Sánchez, Dr. Javier de la Hidalga y Dr. Edgar Reyes por el esmero dedicado a las correcciones y la lectura del presente documento.

Dedicatory

A mis padres: María de los Ángeles Linares Cú y Mario Galindo Gutiérrez porque hemos escalado juntos una cumbre más a pesar de la inclinación de su pendiente, de la neblina y de otros factores que la naturaleza nos puso en el camino hacia la montaña del éxito. Para ustedes mis dos grandes e inseparables amores, como un reconocimiento a su esfuerzo (plasmado en los años de trabajo) y dedicación para hacer de mí una mujer con estudios.

A mi gran familia: amigos y compañeros para aquellos que me adoptaron y a quienes adopté cuando ingresé a la carrera, porque jamás me equivoqué al apostar por la amistad de grandes mujeres y hombres. Para mis hermanos co-sanguíneos: Irasema, Alejandro, Antonio y Adrián. A los muchos amigos que se anexaron a esta lista en mi paso por la maestría, porque hoy por hoy me han regalado una muestra de no haber perdido su esencia como humanos y por el tiempo de sus vidas que no sólo a mí me obsequiaron. Por ayudarme a caminar en los momentos de tropiezo.

A la vida, que me ha dado la oportunidad de estar nuevamente en pie, luchando una batalla más en el capítulo de la supervivencia y sobrevivencia en el planeta. Dándome testimonio feasiente de lo importante que resulta vivirla plenamente. Gracias por demostrarme lo mucho que vale el despertar cada mañana abrir los ojos, poder ver, moverse, oler, hablar, comer, oir, sentir ... porque me ha enseñado lo hermoso que puede ser un día o un segundo mientras se viva con calidad.

Acronyms

BG(s)	Band Gap(s)
BiCMOS	Bipolar CMOS
CMOS	Complementray Metal-Oxide-Semiconductor
CW	Continuous Wave
d	lattice constant or period
EM	Electromagnetic
Er^{3+}	Erbium ion
f	filled fraction
Im	Imaginary part
k	Bloch wave vector
N	Impurity concentration
PB(s)	Photonic Band(s)
PBG(s)	Photonic Band Gap(s)
PBS	Photonic Band Structure
PC(s)	Photonic Crystal(s)
P_p	Radiated power
R	Reflectance
Re	Real part
SE	Spontaneous Emission
Si	Silicon
SiO_2	Silica or silicon oxide
SL(s)	Super Lattice(s)

T	Transmittance
TE	Transversal Electric mode
TM	Transversal Magnetic mode
TMM	Transfer Matrix Method
β	propagation constant
ω	angular frequency
ω_p	plasma frequency
Γ_p	SE rate
1D	One-Dimensional
2D	Two-Dimensional
3D	Three-Dimensional

Contents

List of Figures

Chapter 1

Introduction

In the last fifty years, the developments in solid state science and engineering have increased the research and use of new materials. Researchers have developed innovations in new materials (pures, alloys or artificials) with interesting optical properties. Photonic crystals (PCs) are a new class of artificial materials. Such structures are appropriate for the transfer of information in wave form with minimal loss, to reconstruct a signal. The complexity in bringing together optics and electronics increases, given the need to generate smaller and more efficient devices. This requires the use of advanced technologies on the order of microns and/or nanometers.

Since the invention of the laser, after Einstein's theoretical contribution, the improvements in the application of monochromatic light in telecommunications has been a main goal. Such efforts gave origin to the invention of optical fibers. Nowadays the optical Si fiber is the material commonly used in telecommunications. However the proposal to optimize the data transmission with the use of new structures such as PCs has been around for about twenty years.

On the other hand, when we think about new materials it is important to propose innovations over the industrial working technology with an optimized fabrication processes. Optoelectronics tries to integrate the bipolar and the Complementary Metal-Oxide-Semiconductor (CMOS) technologies, working in the tens of GHz frequency range. Both technologies or their combination (BiCMOS) could be applied to photodiodes, optical fibers, transistors and diverses optical systems [1]. Nowaday the common materials to build these are Si and SiO_2.

This would open the possibility to create signal channels by integrating photonics and electronics, introducing Si in photonic materials.

1.1 Photonic crystals

Yablonovitch and John [2, 3] pioneered the research of a new kind of photonic material. In 1987 they developed three-dimensional periodic structures made of dielectric materials with different permittivities and refractive indexes, stacked alternately. The stack spatial period is known as lattice constant and is on the order of the wavelength of the relevant electromagnetic (EM) waves.

They also realized optical tests to characterize the materials, and analyzed the behavior of photons in the new materials. Given that the new materials display structures similar to the ones known in solid state, they became known as PCs.

PCs are composed at least of two dielectric materials and are classified according to the dimensionality of the stack. The main property of one-dimensional (1D) PCs is the periodicity in one direction, two-dimensional (2D) PCs show periodicity in two directions while three-dimensional (3D) PCs have periodicity along the three spatial directions. All PCs present the photonic band gap (PBG), localized modes in the presence of defects and surface states. Figure 1.1 displays a schematic representation of PC structures.

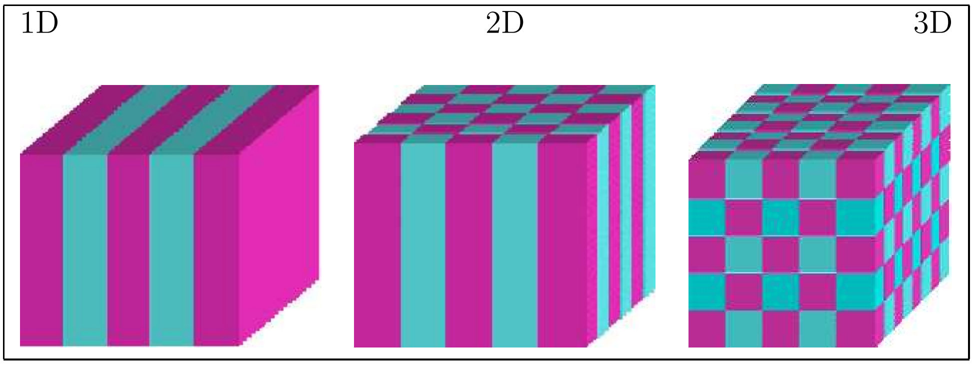

Figure 1.1: PCs in one, two, and three dimensions

The dimensionality of the periodicity is important, because PCs show regions where the propagation of light is forbidden in a certain direction or directions. So far the only structures known without light progation are the

3D PCs. These exhibit a completely forbidden band, in contrast to 1D and 2D PCs.

In this thesis, analysis of PCs was realized using classical theory of electrodynamics, namely Maxwell's equations. The wave equation is reduced to an eigenvalue problem, suitable to be solved using a numerical method.

In this work the simulated stacks are 1D PCs also known as dielectric multilayers or superlattices (SLs).

The macroscopic Maxwell's equations (in cgs units) are [4]:

$$\nabla \cdot \mathbf{B} = 0 \tag{1.1}$$

$$\nabla \cdot \mathbf{D} = 4\pi\rho \tag{1.2}$$

$$\nabla \times \mathbf{E} + \frac{1}{c}\frac{\partial \mathbf{B}}{\partial t} = 0 \tag{1.3}$$

$$\nabla \times \mathbf{H} - \frac{1}{c}\frac{\partial \mathbf{D}}{\partial t} = \frac{4\pi}{c}\mathbf{J} \tag{1.4}$$

where **B** is the magnetic induction field, **D** is called the electric displacement, **E** and **H** are the macroscopic electric and magnetic fields respectively, ρ is the free charge density, **J** represent the current density and finally, c is the speed of light.

Our system is a PC with homogeneous dielectric ingredient materials without free charges and currents.

In the eqs. (1.1) - (1.4) we must specify the relations between the displacement and electric fields and between the magnetic induction and magnetic fields. A good approximation to solve the equations system is to take the fields small enough to eliminate non-linear terms, also assuming that the materials are isotropic and uniform. We have then

$$\mathbf{D}(\mathbf{r}) = \varepsilon(\mathbf{r})\mathbf{E}(\mathbf{r}) \tag{1.5}$$

and for non-magnetic materials, with $\mu = 1$ as in free space, we can set

$$\mathbf{B} = \mathbf{H}. \tag{1.6}$$

For harmonic time-dependence $e^{-i\omega t}$ Maxwell's equations simplify:

$$\nabla \cdot \mathbf{H} = 0 \tag{1.7}$$

$$\nabla \cdot [\varepsilon(\mathbf{r})\mathbf{E}] = 0 \tag{1.8}$$

$$\nabla \times \mathbf{E} - i\frac{\omega}{c}\mathbf{H} = 0 \tag{1.9}$$

$$\nabla \times \mathbf{H} + i\frac{\omega}{c}\varepsilon(\mathbf{r})\mathbf{E} = 0. \tag{1.10}$$

Eliminating **E** from the last two equations, we obtain the master equation for PCs

$$\nabla \times \frac{1}{\varepsilon(\mathbf{r})}\nabla \times \mathbf{H}_\omega(\mathbf{r}) = \frac{\omega^2}{c^2}\mathbf{H}_\omega(\mathbf{r}). \tag{1.11}$$

All 1D and 2D PCs are necessarily anisotropic. On the other hand, 3D PCs can be isotropic for small wave vectors (if constituted from isotropic materials).

In what follows I turn to 1D PCs, the subject of my thesis.

1.1.1 One-dimensional photonic crystals

We suppose that the layers of the 1D PC are homogeneous and isotropic. We assume that EM waves are incident at the structure and study the optical properties (reflectance, transmittance and absorbance). To solve this system we use the Bloch-Floquet theorem.

The relation between EM fields and their characteristic polarizations, for s polarization (**E** perpendicular to the plane of incidence or TE) as well as for p polarization (**H** perpendicular to the plane of incidence or TM) is obtained by means of the boundary conditions, assuming N periods (composed from two different dielectric materials), taking air as the incident medium [5, 6]. The two layers of any period have indexes. This theoretical study is known as Transfer Matrix Method (TMM), that is the numerical method that we use for our computer calculations.

The details of the calculation can be found in many textbooks - for example those by Born and Wolf [5] and Pochi Yeh [6].

The reflectance is the ratio of the energies of the reflected and the incident waves, i. e. the fraction of reflected energy, expressed as

$$R = |r|^2. \tag{1.12}$$

where r is the reflection coefficient.

On the other hand, the radiated power transmitted by the structure, divided by the total radiant energy incident at it, represents the transmittance, given by

$$T = \frac{n_3 cos\theta_3}{n_1 cos\theta_1}|t|^2 \tag{1.13}$$

where n_1 and n_3 are the refractive indexes of medium 1 and 3, θ_1 and θ_3 are the transmitted angle waves of medium 1 and 3, respectively and t indicates the transmission coeficient.

Since there are no materials with null absorption, in order to do the calculation in a realistic way, it is necessary to consider the dissipated energy fraction (absorbance), given by

$$A = 1 - R - T \tag{1.14}$$

where A is the absorbance.

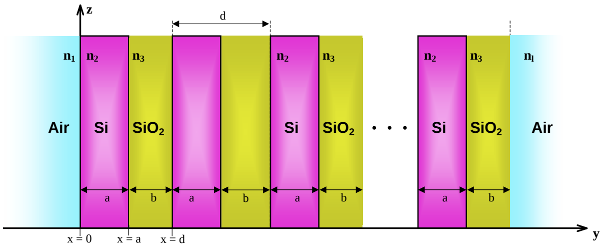

Figure 1.2: Multilayer schematic representation of a Si/SiO$_2$ one-dimensional photonic crystal. There are N periods of the layers bounded by air.

The band structure calculation also can be realized using this TMM. For this it is necessary to determine the Bloch wave vector.

In this case, the system to analyze is an infinite SL composed of two materials with different refraction indexes. The corresponding phase factor is expressed as

$$e^{ikd} = \frac{1}{2}(A + D) \pm \left\{ \left[\frac{1}{2}(A + D) \right]^2 - 1 \right\}^{\frac{1}{2}}, \tag{1.15}$$

where A and D are defined in Ref. [6] and can be expressed in terms of the refractive indexes and widths of the two layers and the propagation constant (β) .

Equation (1.15) gives the dispersion relation between ω, β and k. The Bloch wave vector k can be expressed as

$$k(\beta,\omega) = \frac{1}{d} cos^{-1}\Big[\frac{1}{2}(A+D)\Big] \tag{1.16}$$

where $|\frac{1}{2}(A+D)| < 1$ corresponds to real k and thus to propagating Bloch waves. When $|\frac{1}{2}(A+D)| > 1$ k has an imaginary part k_i so that the Bloch wave is evanescent (corresponding to a forbidden band). The band edges are given by $|\frac{1}{2}(A+D)| = 1$. The dispersion relation between ω and k can be written explicitly for normal incidence ($\beta = 0$) as

$$coskd = cos(k_1 a)cos(k_2 b) - \frac{1}{2}\Big(\frac{n_2}{n_1} + \frac{n_1}{n_2}\Big) sin(k_1 a) sin(k_2 b) \tag{1.17}$$

where $k_i = n_i \frac{\omega}{c}$ with $i = 1, 2$.

This thesis continues a line of research by Halevi and collaborators. In Ref.[7], the authors calculate the optical properties of a 1D PC as a function of impurity concentration for $\omega = 9.1 \times 10^{13}\mathrm{s}^{-1}$; they also calculate the reflectance as a function of the frequency at different temperatures. In Ref.[8], they study the tuning of 2D PCs, proposing variations in temperature (T-tuning) or in impurity concentration (N-tuning). In Ref.[9], they calculated modifications of the PBG when varying an applied electric field in a 2D PC infiltrated with liquid crystal. Results show tuning and also switching. In Ref.[10] they obtained theoretical results for tunable 2D PCs when the temperature range varies from 200K to 290K, with cylinders of InSb in air. A significant result obtained is that because of absorption phononic resonances disappear; also substantial T-tunability of the transmittance was demonstrated. In Ref.[7], the intrinsic carrier density changes are obtained by the same methods showing N-tuning and T-tuning, but for 1D PCs.

We have results for 1D PCs with alternating layers of Si and SiO_2 doped with impurities (n type) with densities from $1 \times 10^{15}\mathrm{cm}^{-3}$ to $3 \times 10^{20}\mathrm{cm}^{-3}$. Here, we only present the most important range of results from $1 \times 10^{19}\mathrm{cm}^{-3}$ to $3 \times 10^{20}\mathrm{cm}^{-3}$. We wish to tune the optical response of the multilayer structure (reflectance) at 1.54μm. Reflectance calculations were realized by the TMM for isotropic layers, assuming an incident monochromatic EM wave with normal incidence at the PC surface. We also show the PBS for an infinite SL, varying strongly the doping concentration in the same range.

1.2 Rare earth ions inside a PC

In the last years the interest in work with rare earth-doped semiconductors has increased, in view of diverse optoelectronic applications [11]. Erbium is a rare earth of high interest because it exhibits state transitions with photon emission in the wavelength of 1.54 μm.

It is well known that for Si optical fibers doped with Er^{3+} ions, light absorption at 1.54μm is very low. Adding Er^{3+} ions to Si produces optical as well as electrical excitations.

Other rare earths currently researched are neodymium (Nd), ytterbium (Yb), cerium (Ce) and terbium (Tb) among others. Nd and Yb work about 1 μm, while Ce and Tb work at visible frequencies.

PCs doped with Er^{3+} can show better results if the host material is also doped with oxygen (O_2) and/or fluor (F) impurities.

A research line for telecommunications focuses on sending several signals at the same time on a single fiber [12], using the wavelength of 1.54 μm, given that Er doped fibers work at this wavelength. The corresponding frequency (1.224$\times$10^{15}Hz) will be used all along this work.

In chapter 3, we study a 1D PC implanted with an erbium ion (Er^{+3}) on ideal conditions, assuming that it emits at the telecomunications wavelength of 1.54 μm.

Here we extend PC research by exploring mainly 3 important aspects: a) The use of a 1D PC (being this the must basic structure) is the simpler PC model to implement in optoelectronic devices. b) Use of PCs to allow and forbid EM waves transmission around 1.54 μm (important for optical telecommunications).

1.3 Spontaneous emission

PCs present the possibility to control or even inhibit the spontaneous emission (SE) inside the PBGs.

It is possible to forbid the propagation of a photon inside a PBG, i. e. to avoid the photon emission by an atom inside the PC for certain frequency bands.

We know that defects can be introduced in a PC, allowing frequencies inside the BG in which the photons can propagate. Also the photon propagation can be allowed or forbidden in a given direction or directions.

In general, SE will give rise to EM wave propagation in the PC. This effect occurs because, when the electron decays from a given energy level to its ground state in the atom, it emits a photon with energy $\hbar\omega$. It is possible to calculate the SE rate using the classical expression for the dipolar radiation. A formula similar to the "Fermi golden rule" can be applied [4]. Such an equation for the emission rate, for an arbitrary inhomogeneous dielectric medium with an embedded atom, was reported by Dowling and Bowden in 1992 [13]. They also applied their theory to a "Dirac comb" [14] SL.

Given the wavelength of interest, we propose to work with a single Er^{3+} ion which emits photons spontaneously at 1.54 μm. Such an ion is introduced into the 1D SiO_2/Si PC structure. We propose to tune the SE by means of doping a given layer with impurities and varying the density of these impurities. The range of doping will be from 1×10^{19}cm^{-3} to the 1×10^{20}cm^{-3}.

Diverse methods exist to modify the dielectric constants of different materials. This work is an extension of the idea of modifying the semiconductor permittivity, assuming that it is dependent on the free carrier concentration. This depends, in turn, on other quantities such as temperature and doping concentration. For simplicity absorption is not considered in the band structure and SE numerical calculations.

A PC's optical properties can be studied by simulation of the structures under certain controlled conditions. This work is focused on simulating two properties, first analyzing the reflectance of a finite 1D PC, and the second is tuning of the SE in an infinite 1D PC. In both cases we analyzed the SL tunability, but for the reflectance the light source is external, while for the SE the source is internal.

The spontaneous emission calculation was realized assuming only one Er^{3+} atom implanted in the PC.

The thesis is organized as follows:

In chapter two, the theoretical conditions for a 1D PC simulation are presented. The reflectance numerical simulation results, considering a SiO_2/Si finite multilayer structure, and the band structure in the first Brillouin zone for an infinite 1D SiO_2/Si PC are shown.

In Chapter three we simulate spontaneous emission of an (Er^{3+}) ion embedded in a 1D PC. Chapter four presents conclusions.

Chapter 2

Tuning of the reflectance

2.1 PCs tuning methods

PCs by now constitute a mature field, with numerous applications. One of these is *tuning*, namely the optical response of the PC is altered by means of some external agent. Such control of the response −for instance reflectance or spontaneous emission− includes the special case of *switching* it on and off. The large number of papers published on the subject of tuning of PCs may be classified as follows. 1) Producing *structural changes* in the PC, without changing the material properties of the ingredients [15]. This has been achieved by miscellaneous methods such as mechanical stress, a piezoelectric material subject to an electric field, insertion of diodes, and the tip of an atomic force microscope. 2)A second way of control is obtained by the incorporation of a *ferroelectric or a ferromagnetic substance* within the PC; an applied electric or magnetic field, respectively, will then alter the photonic band structure and, consequently, the response [16]. 3) Further, two papers exploit the *thermo-optic effect* to tune wave propagation in PC waveguides and channel-drop devices [17, 18]. 4) Infiltration of the PC with a *liquid crystal* −remarkably sensitive to temperature changes, pressure, and applied electric or magnetic fields− is a much favoured approach [19]. 5) In continuation, illumination by an *intense laser beam* can produce small (non-linear) changes in the refractive index of a constitutive material of the PC. Here advantage is taken of the electro-optic or the photorefractive effects in order to tune diverse PC structures [20]. 6)The last category of tuning considered −and the one that concerns us in this thesis− is based on the creation of *electron-hole pairs* in a semiconducting constituent of the PC. This can be accomplished either by heating the semiconductor (T-tuning) or by charge injection (N-tuning) [7, 8, 10, 21–30].

2.2 T- and N- tuning

T-tuning is most effective for narrow-gap semiconductors, such as InSb, that give rise to large densities of free electrons $-$ excited thermally from the valence band to the conduction band. This was shown to lead to dramatic changes in the photonic band structure of InSb cylinders in a square lattice [8]. Similar results were obtained in Ref. [21] , and the possibility of controlling the direction of wave propagation in a Y-shaped, two-dimensional (2D) PC waveguide was proposed [22]. Recently, simulations of T-tuning in 1D [7] and 2D [10] PCs were also performed. And, the tuning of pulses traversing 1D and 2D PCs with defects was reported in Refs. [23] and [24], respectively. Moreover, T-tuning of InAs quantum dots in a PC cavity can enhance or suppress their rate of spontaneous emission [25].

As for N-tuning, the charge injection may be realized either by means of optical excitation or by forward biasing a p-n junction. The latter technique is based on free carrier injection into the intrinsic region of a forward biased p-i-n device [31]. Faster carrier density changes are achieved by embedding a metal-oxide-semiconductor structure in optical devices [32]. Theoretical investigations, mostly on strongly doped n-Si PCs were carried out for 2D photonic band structure [8], for simulation of continuous wave (CW) transmission in 1D [7] and 2D [10] PCs and for transmission of pulses in 1D [23] and 2D [24] PCs with defects. Recently it was also shown that the rate of spontaneous emission of an atom (modeled by a dipole), embedded in a SL, can be substantially altered by N-tuning [26]. On the experimental side, optical excitation was prefered, achieving ultrafast tuning in 2D PCs[27, 28]. Guided modes in PC waveguides were also tuned [29] and it was demonstrated that a nanocavity in a PC can be optically controlled [30].

In this thesis we show that sensitive N-tuning can be achieved in a simple configuration, with technologically important and readily processable materials, and at an important infrared wavelength. The configuration is a 1D PC or SL; the materials are silicon and silicon oxide, and the wavelength is $1.54\mu m$ $-$ widely employed in optical communications (relying on Er-doped optical fiber amplifiers). We have already demonstrated that tuning of the spontaneous emission is feasible for just such a system at the same wavelength [26].

2.3 One-dimensional PC features

In what follows we simulate reflectance measurements, for a n-Si/SiO$_2$ SL, as function of the donor impurity concentration in the Si layers. This concentration, N, is our tuning agent and it is assumed to be high, $N \sim 10^{19}/cm^3$ – which is necessary for achieving sensitive tuning with the wavelength fixed at $\lambda_0 = 1.54\mu m$. Although such high concentrations could be expected to be destructive for a device based on these ideas, we will demonstrate that a judicious choice of the parameters can minimize undesirable absorption. We use the plasma model for a realistic description of the n-Si dielectric constant:

$$\frac{\epsilon(\omega)}{\epsilon_\infty} = 1 - \frac{\omega_{pe}^2}{\omega(\omega + i/\tau_e)} - \frac{\omega_{ph}^2}{\omega(\omega + i/\tau_h)}. \tag{2.1}$$

Here, ϵ_∞ is the high-frequency dielectric constant, $\tau_{e,h}$ are the electron and hole scattering times, and $\omega_{pe,h} = (4\pi n_{e,h}^2 e^2/m_{e,h}\epsilon_\infty)^{1/2}$ are their plasma frequencies. The densities of the electrons n_e in the conduction band and of the (effective)holes n_h in the valence band are related to the impurity concentration N by $n_{e,h} = (n_i^2 + N^2/4)^{1/2} \pm N/2$. Because the intrinsic concentration n_i is very small in comparison to N, actually $n_e \simeq N$ and $n_h \simeq n_i^2/N$. See Ref. [7] of the parameters.

2.4 Reflectance results

Usually, the period of the SL d is chosen to be comparable to the operational wavelength λ_0. If we take $d = 0.73\mu m$, with the Si layers occupying a fraction $f = 0.5$, Fig. 2.1 is obtained for the reflectance. Note that, for $n = 50$ periods, the $R(N)$ curve is initially very steep, with a 70% decrease of the reflectance, which surely is a desirable tuning characteristic. Moreover, if we eliminate the absorption (by substituting $\tau_{e,h} = \infty$ in Eq.(2.1)) the resulting figure is indistinguishable on this scale. On the downside, however, the response is qualitatively dependent on the number of periods. This aspect can be remedied by selecting a much larger period, $d = 7\mu m$, Fig. 2.2. A steep response is seen for $N \simeq 5 \times 10^{19}/cm^3$, which is not much sensitive

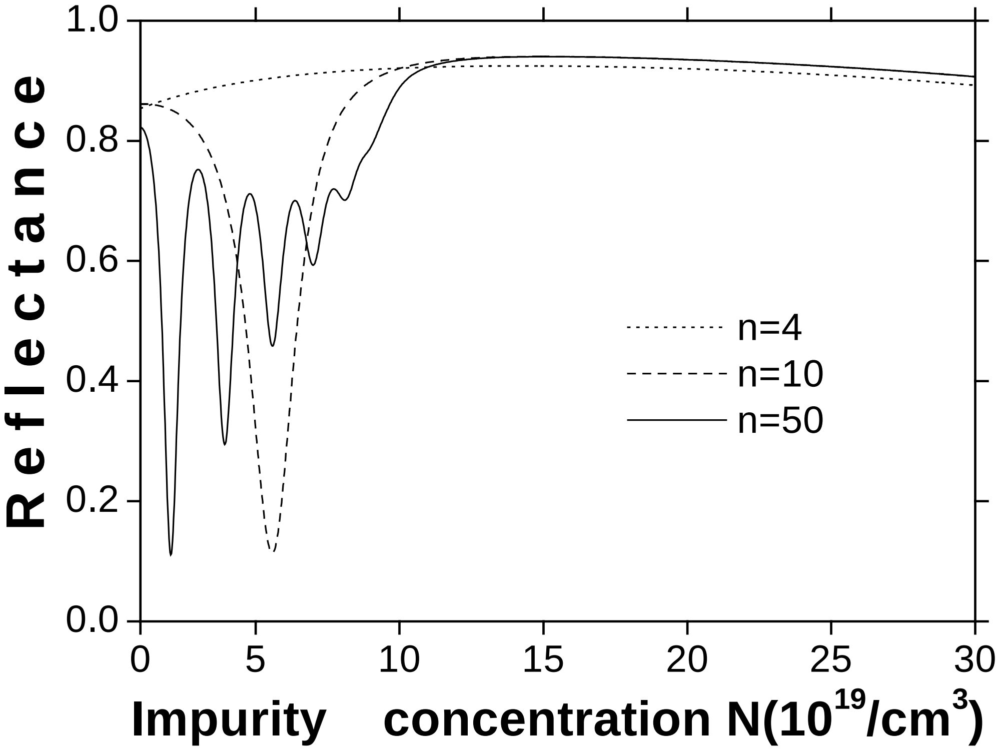

Figure 2.1: Reflectance for a one-dimensional photonic crystal of Si and SiO_2 layers. The silicon layers are strongly doped and we show how the reflectance is tuned by varying the impurity concentration. Four, 10, and 50 periods in the length of the superlattice are considered. The period is $d = 0.73\mu m$.

to either the number of periods or to absorption (bottom panel; in the top panel absorption has been "turned off"). By changing N from 4.14 to $5.74 \times 10^{19}/cm^3$, *switching* is also possible, for the reflectance drops from a high value (0.8 for $n = 10$) to zero. For greater values of the concentration, though, the reflectance is strongly impacted by dissipation, so that the regime $N > 6 \times 10^{19}/cm^3$ is unsuitable for tuning.

The three almost vertical lines in Fig. 2.2(a), at $N \simeq 5$, 23 and $31 \times 10^{19}/cm^3$, have the appearance of band edges that are characteristic of $R(\omega)$ plots. To convince ourselves that they are, indeed, band edges −although in the $R(N)$ representation (with ω as a parameter)− let us look at two different renditions of the photonic band structure in Fig. 2.3. Here, for the unlimited PC, the frequency ω is plotted as function of the Bloch wave vector k (N being a parameter) in part (a) and as function of the impurity density N (now with k as the parameter) in part (b). The heavy horizontal line represents the frequency $\omega_0 = 2\pi c/\lambda_0$. As Fig. 2.3(a) clearly shows, this line lies completely in the band gap for $N \lesssim 3 \times 10^{19}/cm^3$ − between the curves "3" above and below the ω_0 line. For this reason, in this range of N the light must be completely reflected in the ideal, absorptionless and infinite SL − as is suggested by Fig. 2.2(a). For $N = 5 \times 10^{19}/cm^3$ the lower curve "5" already intersects the ω_0 line, thus making optical modes available for propagation. Fig. 2.3(b) confirms this reasoning and, moreover, the left edge ($k = \pi/d$) of the central band crosses the line ω_0 at the precise value of the transition from the low-N stop band to a pass-band − at $N = 4.9 \times 10^{19}/cm^3$. For greater N values Fabry-Perot oscillations of the reflectance are apparent in Fig. 2.2(a) and, in a damped form, also in Fig. 2.2(b). Entirely similar considerations are applicable to the band edge at $N \simeq 31 \times 10^{19}/cm^3$ in Fig. 2.2(a). And a glance at the lower curve "30.7" in Fig. 2.3(a) reveals that it is just tangent to the ω_0 line − which fixes the band edge at $30.7 \times 10^{19}/cm^3$. As for the band edge at $N \simeq 23 \times 10^{19}/cm^3$ in Fig. 2.2(a), we note that in Fig. 2.3(a) the curve "20" crosses the ω_0 line, while this line lies between the curves "30", namely in a band gap. The precise position of the band edge is given by the intersect, in Fig. 2.3(b), of the right side edge of the central band (for $k = 0$) with the ω_0 line − $N = 23.6 \times 10^{19}/cm^3$.

Why is the first stop-band, at $N \lesssim 5 \times 10^{19}/cm^3$, quite insensitive to absorption, while the second stop-band, centered at about $27 \times 10^{19}/cm^3$, suffers strong attenuation? This is readily explained by the fact that, as N increases, so does the scattering of the free electrons from the impurities. Mathematically, this scattering manifests itself in smaller collision times $\tau_{e,h}$

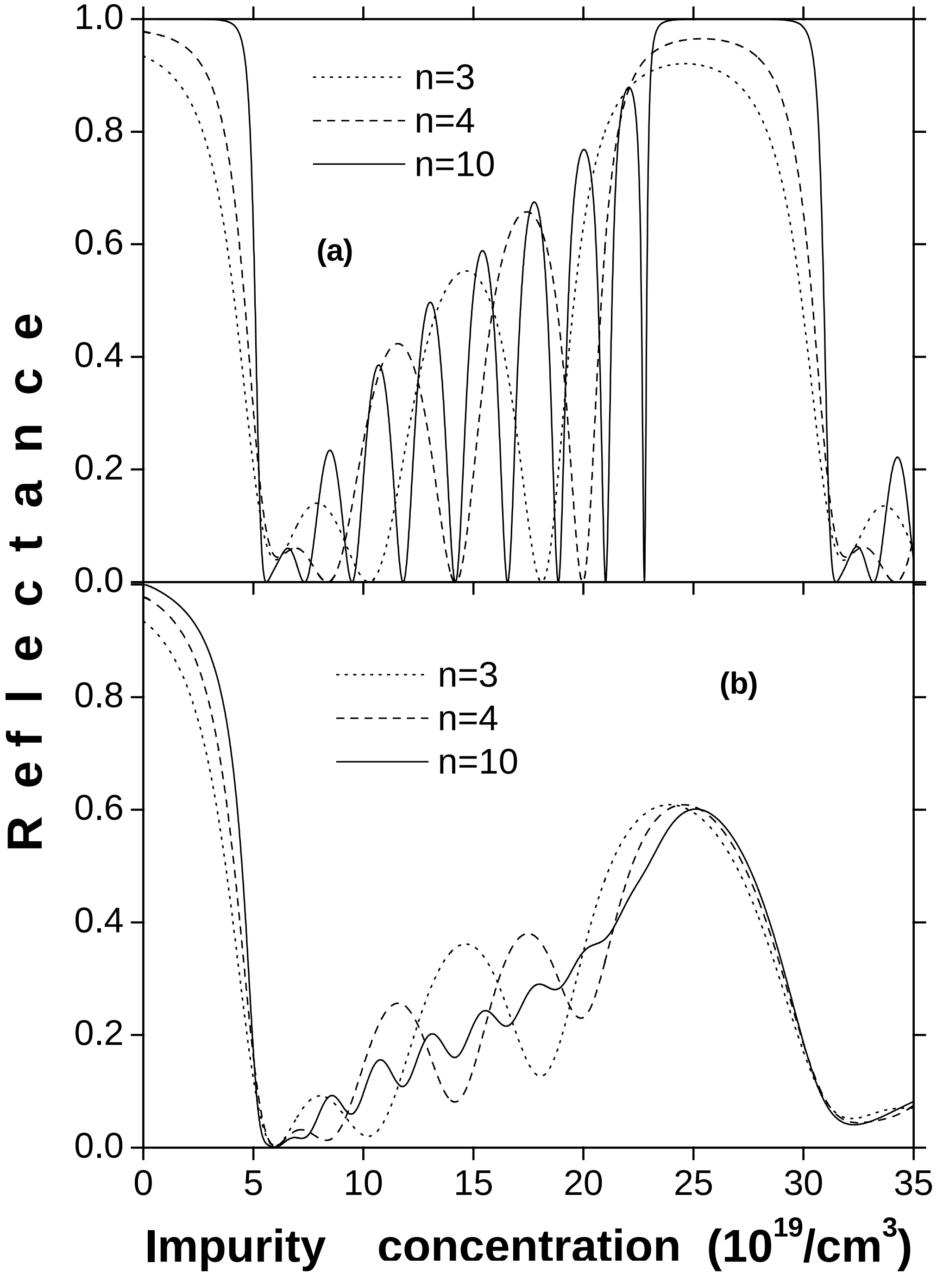

Figure 2.2: As in Fig. 2.1 for a period $d = 7\mu m$, now considering superlattices three, four, and 10 periods long. Absorption has been turned off in (a) and turned on in (b). Note that the band edge at $N \simeq 5 \times 10^{19}/cm^3$ is appropriate for tuning.

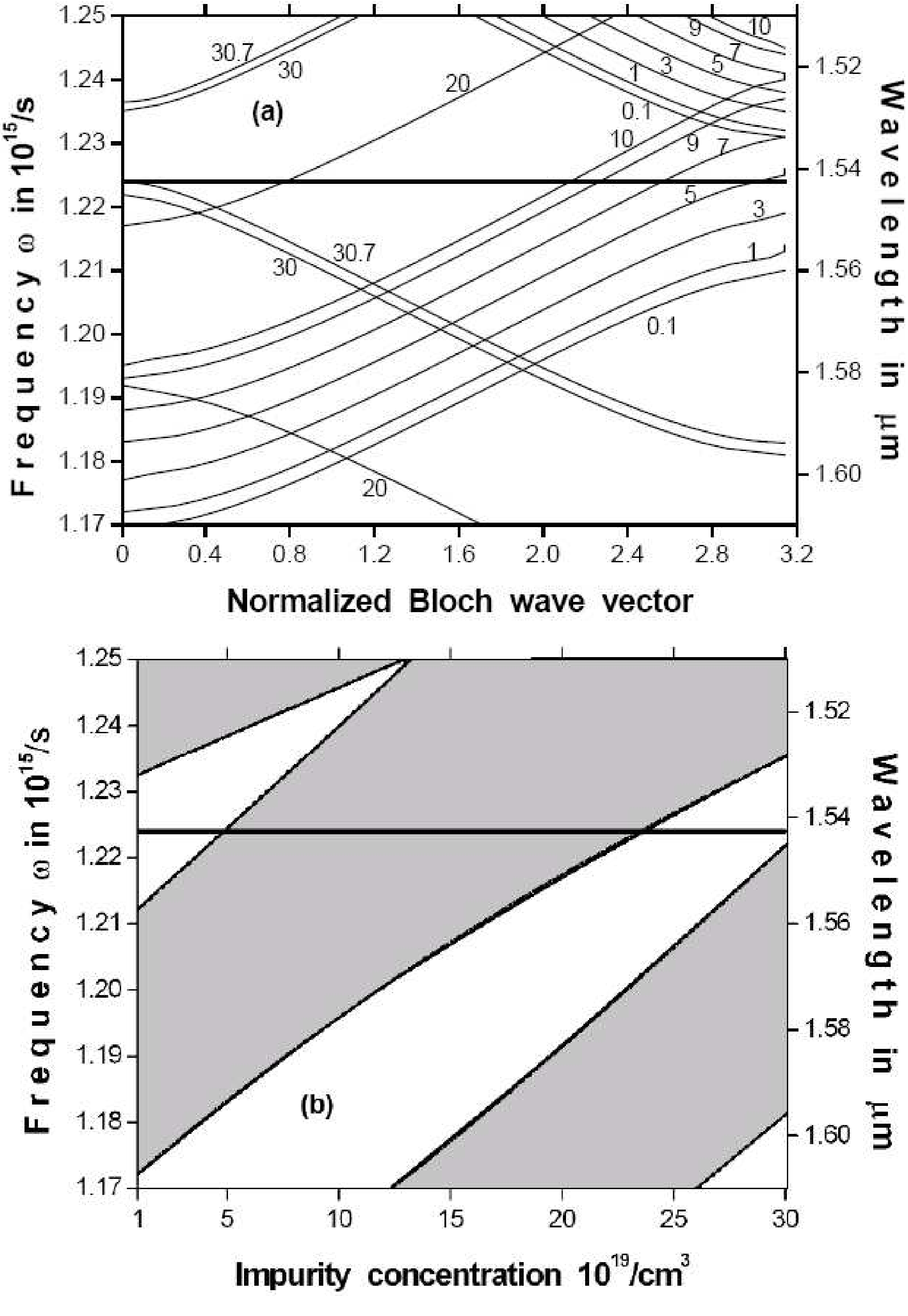

Figure 2.3: Band structure for the (infinite) photonic crystal considered in Fig. 2.2(a). The frequency (wavelength) is plotted on the left (right) side axis as function of the normalized Bloch vector kd (with N as parameter) in part (a) and *vice versa* in part (b). In (a), the numbers next to each line are the values of N in $10^{19}/cm^3$. The horizontal lines mark the frequency corresponding to the wavelength of $1.54\mu m$.

in Eq. (2.1).

We have thus shown that both tuning and switching of the reflectance is possible in a Si/SiO$_2$ one-dimensional PC at the technologically important wavelength of $1.54\mu m$. This could be accomplished by either optical or electrical charge injection, varying the impurity density at $N \sim 10^{19}/cm^3$, even with a small number of PC periods. In the case of electrical tuning a unit cell of four Si layers −p-type, intrinsic, n-type, and oxide− could be advantageous. The first three layers would form a p-i-n diode and would serve to modify the carrier concentration, while the oxide layer would increase the dielectric contrast. Such tuning of the reflectance in PCs could have a positive impact on silicon optical devices such as waveguides, modulators, and laser cavities.

So far we have only analyzed the 1D PC optical response by exposing it to an electromagnetic wave or an external stimulus. In the next chapter we analyze the SE response from multilayer structures considering an internal excitation source.

Chapter 3

Tuning of the spontaneous emission

Is it possible to vary spontaneous emission SE *actively* − in real time? The complete idea seems to involve a contradiction of terms: "spontaneous" implies a process that is inherent to the emitting atom, independent of experimental conditions! Nevertheless, in a pioneering paper [33], Purcell pointed out that SE is altered if the radiated field is constrained to satisfy a set of boundary conditions. In other words, the lifetime of an excited atomic state changes if the atom is located in a material environment, rather then radiating in free space. The rate of SE can be inhibited (and even prohibited) or enhanced, depending on the modal density (or density of states). *If now the external conditions are varied on the time-scale of the excited state's lifetime, then we can expect that the natural process of SE becomes manipulable in real time.* Is this feasible?

3.1 Photon emission

Let us consider three types of emitters. (a)*Rare earth ions.* In Er^{3+} the transition $4I_{13/2} \rightarrow 4I_{15/2}$, involving f-shell electrons, gives rise to emission at the important communications wavelength $\lambda_0 = 1.54\mu m$. The radiative lifetime (with the ions implanted in glass) is [34] $\tau = 22ms$. (b)*Nanoparticles (quantum dots).* These are frequently $II-VI$ or $III-V$ semiconductor compounds such as CdSe; they have been implanted in opal-type PCs [35]. Also, silicon nanocrystals have been implanted in silica [36]. Such quantum dots emit in the visible or near infrared; the lifetimes vary over many orders of magnitudes and can be as long as $\sim 10ms$. (c)*Recombination in semiconductors.* The radiative lifetime due to recombination of photo-excited electrons and holes varies widely among semiconductors and depends strongly on the impurity density. For instance, with a density of $10^{17}/cm^3$ of majority carriers, the minority carrier lifetime in Si, Ge, and GaP is on the order of a ms. For intrinsic Si and Ge it is, respectively, $4.6h$ and $0.61s$ [37]. Next, are the temporal scales of tuning compatible with these lifetimes?

3.2 Optical tuning processes

To answer this question, we discuss four possibilites of tuning of the optical response. (A)*Manipulation of the free-carrier density in semiconductors.* The mechanisms of thermal excitation and doping in PCs have been explored in a series of papers [7, 8, 10, 21, 22, 38, 39]. In particular, we found that the transmission of light through a one-dimensional (1D) PC of alternating Si/SiO_2 layers can be sensitively tuned at the wavelength $1.54\mu m$, [39] mentioned in (a). The intensity of high photoexcitation applied to semiconductors can be modulated as rapidly as the laser beam can be pulsed (repetition rates $\lesssim 1ns$). An even more rapid band-edge tuning, in a 2D silicon PC, was achieved by means of $0.3ps$ pulses [27]. And the response time of forward biasing at heterojunctions is $\sim 1ns$ [40]. (B)*Tuning of liquid crystal-infilled PCs* is a very active field, recently reviewed in Ref. [41]. Such tuning may be performed by changing the temperature or by applying a variable electric field, or by shining on pulsating high-intensity light; the response time is on the order of 1ms. We quote a few notable papers [9, 42]. (C)*Employing the thermo-optic effect.* Very recently, Vlasov et al [17] have taken advantage of this effect to tune, in real time, the group velocity of waves propagating in a PC waveguide. The time-scale of the tuning was $0.1\mu s$. (D) *Nonlinear modulation of the refractive index of an insulator.* To quote Yablonovitch [43], "ideally, in nonlinear optics, we regard the refractive index of a medium to be a time-variable function totally under the control of the experimentalist". With solid state, (mode locked) pulsed lasers it is possible to achieve repetition rates as small as $\sim 1ns$ with fs pulses [44].

As we see from the list (A) - (D), the *slowest* tuning agent considered varies on the time scale of 1ms. Then, comparing with the lifetimes for SE in the examples (a) - (c), we note that the *quickest* emission occurs also in about 1ms. Hence, we come to the conclusion that external intervention in the process of SE should be feasible. We expect the rate of emission to depend in an important way on the details of the tuning agent. To quantify this problem we assume that the radiating atom is embedded in a dielectric medium whose permittivity ϵ is being dynamically tuned by some unspecified mechanism. If the temporal dependence $\epsilon = \epsilon(t)$ is given $-$ what is the corresponding rate of SE?

We are not aware of any measurement of the SE by an atom in a dynamically varying host medium. And no theory is available, either, to calculate the rate of emission if $\epsilon = \epsilon(t)$. Hence, in this thesis we will *not* concern ourselves with SE in real time. Rather, we will focus on a specific example that demonstrates appreciable dependence of the SE rate on an external agent of tuning. PCs [45] are often characterized by sharp photonic band edges and are, therefore, singularly attractive choices for hosting the radiating atom. This is true because *the PC can be designed so as to have one of its band edges approximately coincide with the frequency of emission.* Then a modest variation of the tuning agent is expected to produce a sizeable change in the emission rate. Regarding the choices (a)-(c) and (A)-(D) discussed above, we select the (a)-(A) combination. Specifically, this thesis is concerned with the simulation of SE by Er^{3+} ions embedded in a 1D PC of alternating Si and SiO_2 layers [46]. These materials have been selected because of their ease of fabrication, technological importance, and large dielectric contrast. The Er ions are chosen because they emit at the near-infrared wavelength $\lambda_0 = 1.54\mu m$, very important for communications by optical fibers. We assume that the Si layers are strongly doped with impurity donor atoms. The concentration of these impurities is varied externally $-$ and this is the tuning agent commented on above. Presumably, the mechanism would be carrier injection $-$ either photoexcitation or forward biasing; the specifics are of no consequence for the considerations that follow. For highly extrinsic Si, the density of free electrons in the conduction band is practically equal to the donor density. The tuning of these densities modulates the dielectric constant of the semiconductor and this, in turn, shifts the photonic band edges. We then conclude that the *tuning of the charge injection modulates the density of states available to the radiating atom.* This explains the idea behind tuning of the SE rate for the particular example considered.

The semiconductor layers of the PC are modeled as a plasma of free electrons in the conduction band and free holes in the valence bands. The density of these, as function of the donor density N (and no acceptors) is [47]

$n_{e,h} = [\mathrm{N}^2 + n_i^2(T)]^{1/2} \pm \mathrm{N}/2$ where the intrinsic density $n_i(T)$ is very small in comparison to N. The corresponding electron and hole plasma frequencies are $\omega_{pe,h} = (4\pi n_{e,h}e^2/\epsilon_\infty m_{e,h})^{1/2}$. Here ϵ_∞ is the high-frequency dielectric constant equal to 11.7 for Si. We use $m_e = 0.26m_0$, where m_0 is the true electron mass. Also, the conductivity effective mass for holes (m_h) can be obtained from the effective masses of the light (m_{lh}) and heavy (m_{hh}) holes: $m_h = m_{hh}(1 + r^{3/2})/(r + r^{3/2})$, where $m_{hh} = 0.49m_0$ and $r = m_{hh}/m_{lh}$ [48]. The plasma model for the dielectric function takes into account absorption:

$$\epsilon(\omega) = \epsilon_\infty\{1 - \omega_{pe}^2/[\omega(\omega + i/\tau_e)] - \omega_{ph}^2[\omega(\omega + i/\tau_h)]\} \tag{3.1}$$

The scattering times τ_e and τ_h are gotten from the carrier mobilities: $\tau_{e,h} = m_{e,h}\mu_{e,h}/e$ with $\mu_{e,h}$ derived from empirical models that take into account phonon and impurity scattering [49].

3.3 Spontaneous emission results

In Fig.3.1 we plot the real and imaginary parts of Eq.(3.1) as function of the donor concentration N. The circular frequency has been fixed at $\omega = \omega_0 = 1.224 \times 10^{15}/s$, corresponding to the emission wavelength of interest $\lambda_0 = 1.54\mu m$. Re ϵ and Im ϵ change rapidly for N $\gtrsim 10^{19}/cm^3$; while Re ϵ decreases, Im ϵ increases with N. We are thus confronted with opposing demands. On the one hand, it is desirable to have N large enough for the plasma frequency to reach values $\omega_p(\mathrm{N}) \lesssim \omega_0$ (see inset of Fig.3.1) where the tunability is largest. On the other hand, we also wish to keep absorption in check. As a reasonable compromise, we limit the impurity density to the range $10^{19} \leq \mathrm{N} \leq 10^{20}/cm^3$ where, for the upper limit, Im $\epsilon \simeq 0.0046$ Re ϵ. Henceforth, we will take into account only the real part of $\epsilon(\mathrm{N})$. We note that similar models were used for tuning the band structure and reflectance in 1D and 2D PCs [7, 8, 10, 21, 22, 38, 39]. For effective Bragg diffraction the period d should be of the same order as the wavelength ($d \sim \lambda_0 \sim \lambda_p = 2\pi c/\omega_p$). We have chosen $d = 0.73\mu m$ and layers of equal thickness. Using $\epsilon_1 = 2.09$ [48] for the silica layers and ϵ_2 given by the *real part* of Eq.(3.1) for the silicon layers, we obtain the band structure shown in Fig.3.2. At low frequencies ($\omega \lesssim \omega_p$), a forbidden gap just below the first band appears in the band structure. Because the lower edge of the first band approximately coincides with ω_p, this gap is associated with the fact that for $\omega \lesssim \omega_p$, Re $\epsilon < 0$ and light cannot propagate in the semiconductor. The first band is the most

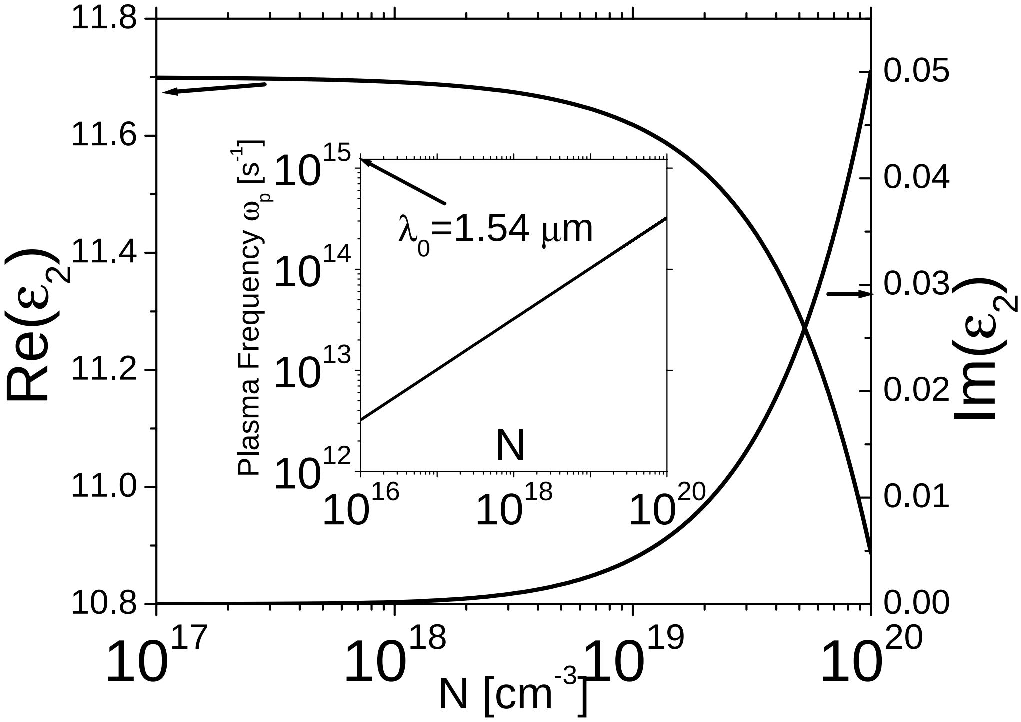

Figure 3.1: Real (left axis) and imaginary (right axis) part of dielectric function of Si as function of impurity concentration. The wavelength is fixed at $\lambda_0 = 1.54\mu m$. The electron plasma frequency is shown in the inset. The arrow points at a hypothetical plasma frequency $2\pi c/\lambda_0$.

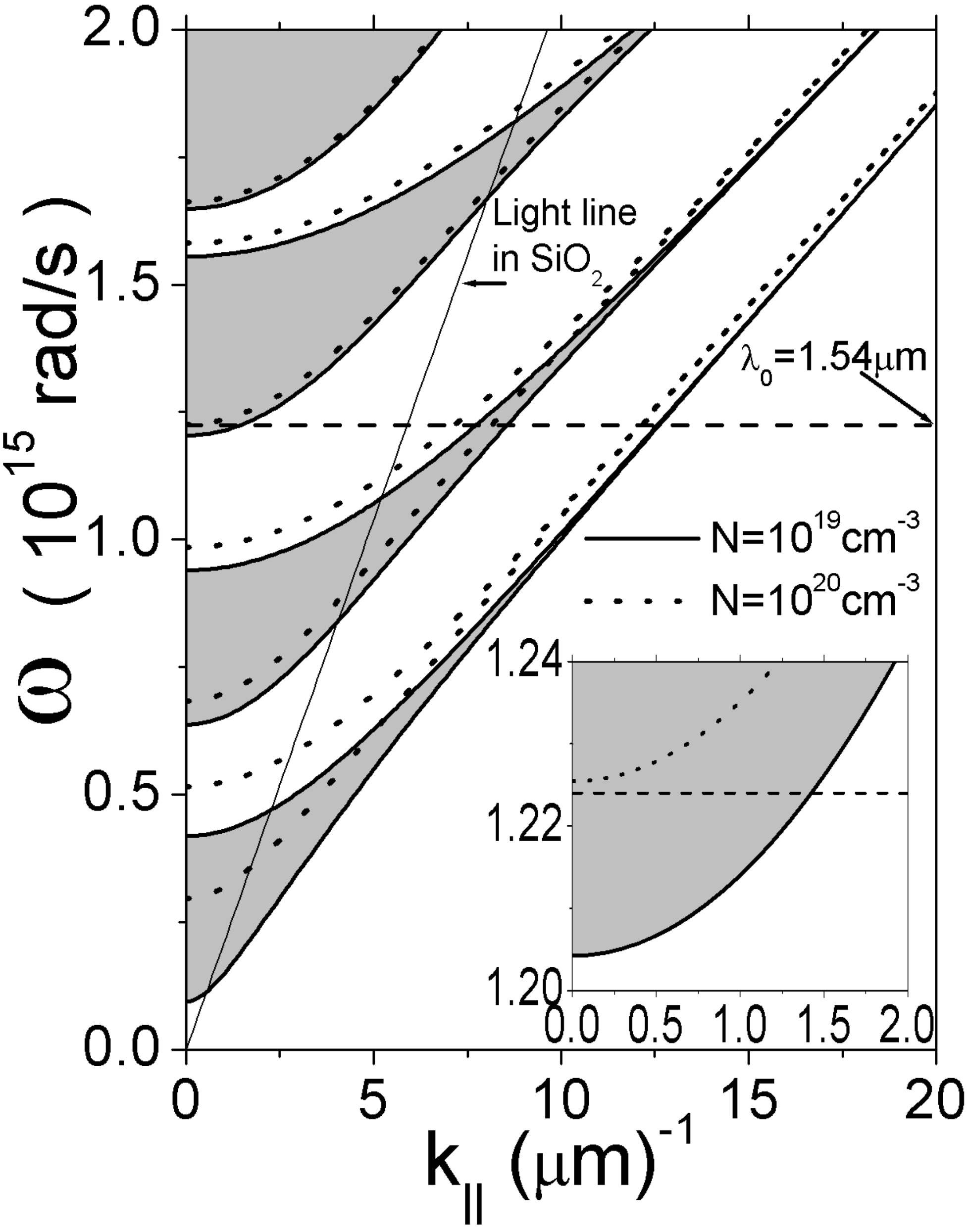

Figure 3.2: TE band structure of a one–dimensional PC with period $d = 0.73\mu m$. Alternating Si and SiO_2 layers have equal widhts. Two values of the electron concentration are considered: N = 10^{19} and $10^{20}/cm^3$. Gray areas correspond to allowed bands for the lower concentration. For the higher concentration, only the band edges are shown (dotted). In the inset, the lower band edges of the third band are amplified for both concentrations.

sensitive to change in N because $\omega \sim \omega_p$. The PC considered was designed to give rise to an on–axis band edge around $\lambda = 1.54\mu m$, see the inset in Fig. 3.2. Thus, when N = $10^{20}/cm^3$ the lower edge of the third band is just above $\omega_0 = 1.224 \times 10^{15}/s$ (corresponding to $\lambda_0 = 1.54\mu m$). For this frequency then, the *radiative* density of modes (with $k_\parallel < \omega/c$) vanishes and there can be no SE. On the other hand, if N = $10^{19}/cm^3$, the frequency $\omega = 1.224 \times 10^{15}$ is located within the third allowed band and, consequently, the radiative density of modes is finite and radiation *can* occur. In Ref. [50] it was found that the SE changes abruptly at the on–axis band edges if the radiating atom is located at an antinode of the modes.

Now we proceed to calculate the rate of SE of an atom hosted by the above described PC. Glauber and Lewenstein [50] have developed a modal quantum electrodynamical theory for the SE rate of an atom embedded in an inhomogeneous dielectric medium, characterized by an arbitrary, position-dependent dielectric function $\epsilon(\mathbf{r})$. A similar, classical theory, was derived by Dowling and Bowden [13], who replaced the two-level atom by a dipole (moment $\boldsymbol{\mu}$) oscillating with the frequency $\omega_0 = (E_2 - E_1)/\hbar$. It is important to observe that the two theories [13, 50] are equivalent because the Wigner-Weisskopff approximation, namely weak coupling of the emitted light to the atom, was assumed in Ref. [50]. This, in fact, corresponds to the situation observed in most experiments of SE. The main result of Dowling and Bowden [13] is the radiated power

$$P_p = \pi^2 \omega_0^2 \int d\mathbf{k} |\mathbf{a}_{\mathbf{k}p}(\mathbf{r_0}) \cdot \boldsymbol{\mu}|^2 \delta(\omega_{\mathbf{k}p} - \omega_0), \tag{3.2}$$

where the index p stands for TE or TM polarization, $\omega_{\mathbf{k}p}$ are the frequency eigenvalues, $\mathbf{a}_{\mathbf{k}p}(\mathbf{r_0})$ are the vector potential eigenvectors evaluated at the atom's position, the Dirac-delta function takes care of energy conservation, and the integration is over all normal modes for a given polarization. The SE rate is, simply, $\Gamma_p = P_p/\hbar\omega$.

Very recently, we have applied Eq.(3.2) to the calculation of the emission rate by an atom embedded in an (undoped) 1D PC [14, 51]. Here we investigate the variation, with impurity concentration, of Γ_p for the Si/SiO$_2$ PC described above. In Fig. 3.3 we show the rate of emission as a function of the emitter's position for several carrier concentrations. The decay rate is normalized to the rate of emission in vacuum ($\Gamma/\Gamma_0 = P/P_0$). It is seen that the tunability is considerably greater for an ion embedded in the SiO$_2$ (white background), than it is for an ion in the Si (grey). For dipoles oriented

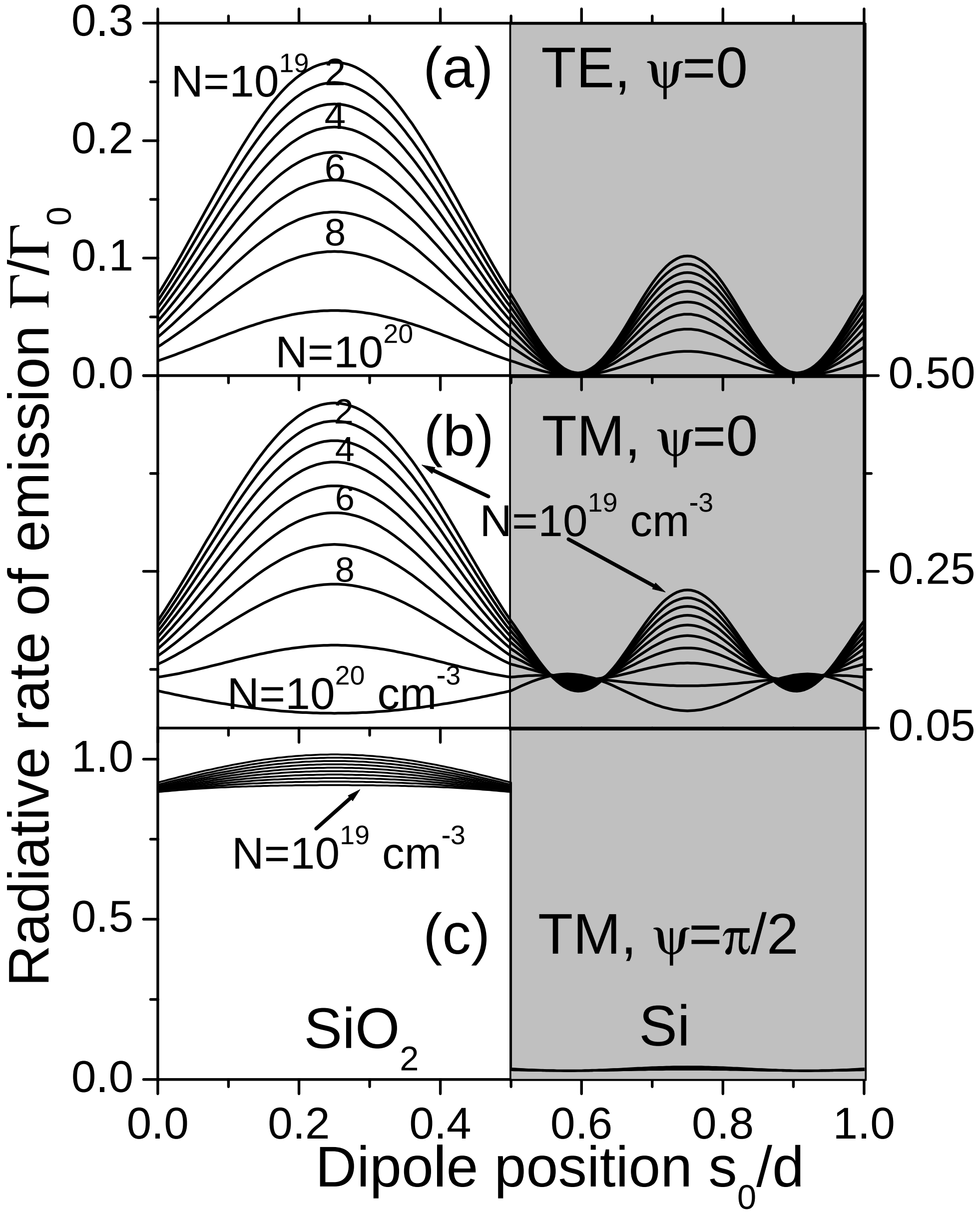

Figure 3.3: Radiative contribution to the rate of spontaneous emission by an Er ion (at $\lambda = 1.54\mu m$) implanted in a Si/SiO$_2$ one–dimensional PC. The rate of emission is normalized with that in air and is plotted as function of the donor impurity concentration and of the ion's position in the SiO$_2$ (left) and Si (right) layers. (a) TE modes, (b) TM modes for dipole parallel to the interfaces, and (c) TM modes for dipole perpendicular to the interfaces.

parallel to the interfaces, the rate of emission into TE modes, Fig.3.3(a), is very sensitive to N. When the donor concentration of Si is $10^{20}/cm^3$ there is no radiative mode because the lower edge of the third band is slightly above the frequency of the spontaneously emitted light. Thus, for this carrier concentration, the radiative contribution to the rate of emission vanishes for any position of the atom. Decreasing the carrier concentration, the rate of emission becomes finite when the lower edge of the third band shifts to frequencies that are below $1.224 \times 10^{15} s^{-1}$ (see the behavior of the on–axis band edge near $\lambda = 1.54 \mu m$ in Fig. 3.2). This means that the emitted light can now couple to radiative modes. The emitter's position at which the rate of emission is most sensitive to changes in the carrier concentration is $s_0 = 0.25$ (at the middle of the SiO_2 layer). The antinodes of the electric-field at the lower band edges indeed coincide with the middle of the low-index layers, as found in Ref. [14]. If $\boldsymbol{\mu}$ forms an angle ψ with the interface, then Γ plotted in Fig. 3.3(a) must be multiplied by $cos^2\psi$.

Consider an excited Er ion at the middle of a SiO_2 layer of a PC with $N = 10^{19}/cm^3$. It would radiate TE–polarized light at a rate $\Gamma \simeq 0.27\Gamma_0$. If, now, the carrier concentration is raised abruptly to $10^{20}/cm^3$, the radiative TE–polarized emission will be prohibited. It is notable that this *switching* occurs when the dielectric function of Si suffers a change of only 6% (see Fig. 3.1). On the other hand, a *gradual* variation of the free-electron concentration from 10^{19} to $9 \times 10^{19}/cm^3$ would result in *tuning* of the SE. In contrast to the emission into radiative modes, the rate of emission into evanescent modes (not shown in Fig. 3.3) is much less sensitive to change in carrier concentration.

For TM polarization, two independent orientations (parallel and perpendicular to the interfaces) contribute to the SE. For dipoles parallel to the interfaces [$\psi = 0$, Fig. 3.3 (b)], the radiative contribution to the SE presents considerable change when the carrier concentration varies from 10^{19} to $10^{20}/cm^3$. The radiative rate of emission, however, never vanishes because the Brewster effect gives rise to closing of the band gaps for $0 < k_\parallel < \omega/c$. When the dipole is perpendicular to the interfaces [$\psi = \pi/2$, Fig. 3.3 (c)], the coupling of the light to the dipole is quite weak; therefore, the rate of emission is not very sensitive to changes in the carrier concentration. Also, the total rate of emission is discontinuous across the interfaces. This is a result of the discontinuity of the component of the electric field normal to the interfaces.

The explicit dependence of the emission rate on the impurity density is

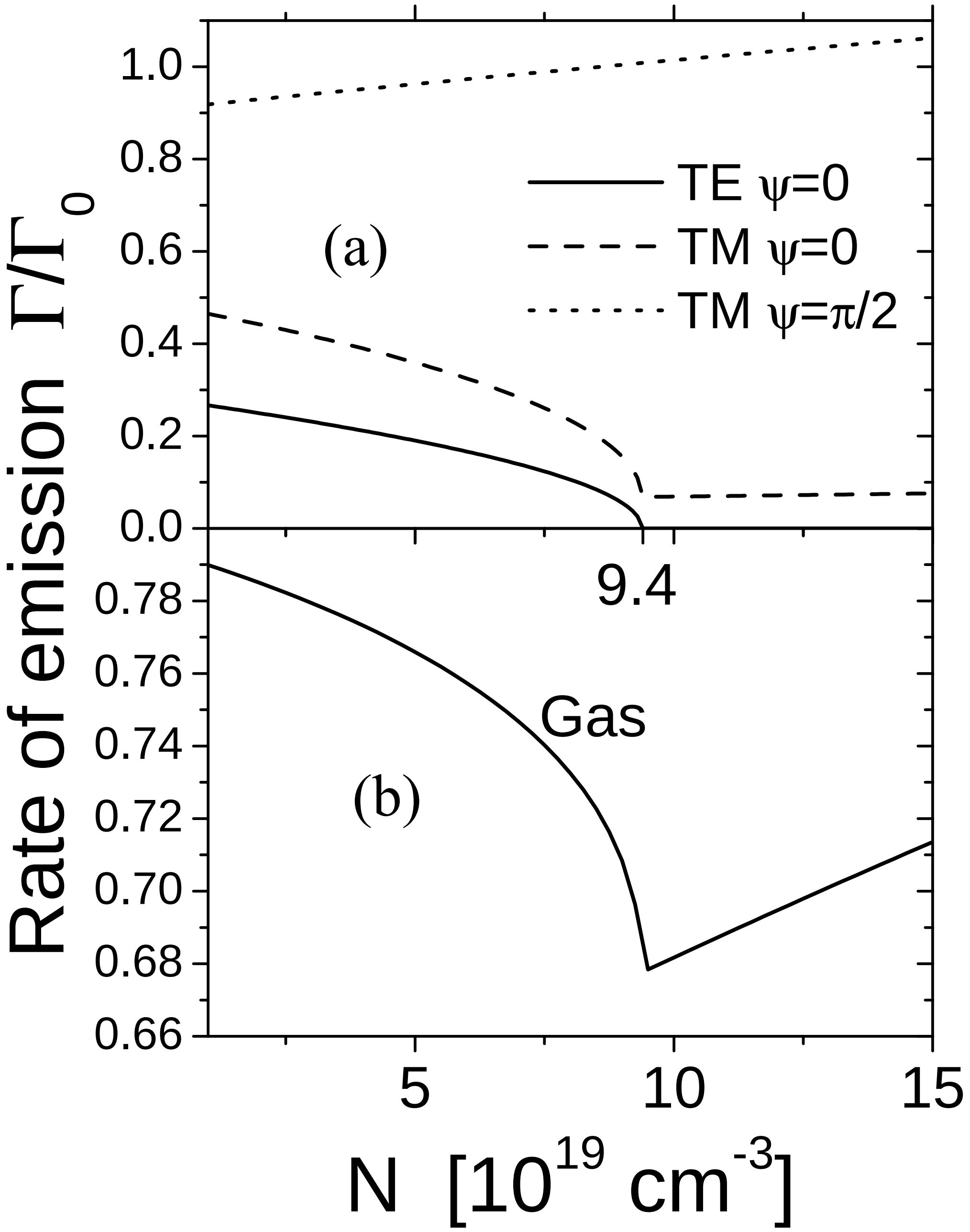

Figure 3.4: Normalized rate of spontaneous emission by an Er ion as function of the impurity density in the layers. (a) The radiating ion is located at the center of SiO_2 the layer; note that for TE polarization $\Gamma = 0$ for N $\geq 9.4 \times 10^{19}/cm^3$. (b)Average rate of SE (per ion) for Er ions evenly distributed in the layer.

displayed in Fig. 3.4. In part (a) the emitter is positioned in the middle of a silica layer. If the dipole moment is parallel to the interfaces, we observe considerable tunability for both polarizations, and the TE component strictly vanishes for N $\cong 9.4 \times 10^{19}/cm^3$. The discontinuity in the slope $d\Gamma/d\mathrm{N}$ at this concentration persists even for a uniform distribution of the donors in the SiO_2 layer, Fig. 3.4 (b). Here we averaged over all the dipole positions and orientations and over the two polarizations.

Chapter 4

Conclusions

We found the optimal filled fraction and period size for a 1D PC system demonstrating tuning and switching.

We have thus shown that both tuning and switching of the reflectance is possible in a Si/SiO$_2$ one-dimensional photonic crystal at the technologically important wavelength of $1.54 \mu m$. This can be accomplished by charge injection, varying the impurity density at $N \sim 10^{19}/cm^3$, even with a small number of PC periods.

We have calculated the rate of SE of an atom embedded in a tunable 1D PC. We designed it so that it has a band edge near the frequency of the spontanously emitted light corresponding to the important wavelength $\lambda = 1.54\mu$m. Therefore, we obtain considerable sensitivity of the radiative SE on the donor impurity density, especially when the emitter's position coincides with an antinode of the normal modes. The results presented are a demonstration, through an example, of the idea that it should be possible to intervene *actively* in the process of SE. As discussed in this thesis, in principle there are many other possibilities for manipulating the relaxation of an atom via photon emission. We believe that dynamic alteration of SE is feasible experimentally. This could have important consequences for sources of light such as LEDs and lasers.

We found a good agreement in the results shown for the reflectance, compared with the ones obtained for the PBSs. The BGs for both cases show a precise match, despite the fact that the SL is finite in the first case and infinite in the second.

One advantage is that all the process is compatible with the bipolar and CMOS technologies, because the size dimensions and design rules are the same for the last mentioned technologies and PCs.

Bibliography

[1] *Silicon Photonics*, eds. L. Pavesi and D. J. Lockwood, Topics in Applied Physics **94**, Springer (2004).

[2] E. Yablonovitch, Phys. Rev. Lett. **58**, 2059 (1987).

[3] S. John, Phys. Rev. Lett. **58**, 2486 (1987).

[4] L. I. Schiff, *Quantum mechanics*, 3rd ed. McGraw - Hill (1968).

[5] M. Born, and E. Wolf, *Principles of Optics*, 5th ed. Pergamon Press (1975).

[6] P. Yeh, *Optical Waves in Layered Media*, Wiley (1976).

[7] A. S. Sánchez and P. Halevi, J. Appl. Phys. **94**, 797 (2003).

[8] P. Halevi and F. Ramos-Mendieta, Phys. Rev. Lett. **85**, 1875 (2000).

[9] P. Halevi, J. A. Reyes-Avendaño, and J. A. Reyes-Cervantes, Phys. Rev. E **73**, 040701R (2006) and references therein.

[10] J. Manzanares-Martínez, F. Ramos-Mendieta, and P. Halevi, Phys. Rev.B **72**, 035336 (2005).

[11] J. F. Digonnet *Rare-Earth-Doped Fiber Lasers and Amplifiers*, 2nd ed. CRC Press, (2001).

[12] Rüdiger Paschotta, *Photonic Crystal fibers*, http://www.rp-photonics.com/photonic_crystal_fibers.html, (2006).

[13] J. P. Dowling and C. M. Bowden, Phys. Rev. A **46**, 612 (1992).

[14] A. S. Sánchez and P. Halevi, Phys. Rev. E **72**, 056609 (2005).

[15] S. Iwamoto, S. Ishida, Y. Arakawa et al, Appl. Phys. Lett. **88**, 011104 (2006); I. Märki, M. Salt, and H. P. Herzig, Opt. Exp. **14**, 2969 (2006) and references therein.

[16] J. Zhou, C. Q. Sun, K. Pita et al, Appl. Phys. Lett. **78**, 661 (2001) and references therein.

[17] Y. A. Vlasov, M. O'Boyle, H. F. Hamann et al, Nature **438**, 65 (2005).

[18] T. Asano, W. Kunishi, M. Nakamura et al, *Elect. Lett.* **41**, 37 (2005).

[19] D. McPhail, M. Straub, and M. Gu, Appl. Phys. Lett. **86**, 051103 (2005) and **87**, 091117 (2005);

[20] A. Haché, and M. Bourgeois, Appl. Phys. Lett. **77**, 4089 (2000); Y. Yi, P. Bermel, K. Wada et al, Appl. Phys. Lett. **81**, 4112 (2002) and references therein.

[21] C. S. Kee and H. Lim, Phys. Rev. B. **64**, 121103 (2001).

[22] H. Takeda and K. Yoshino, Opt. Comm. **219**, 177 (2003).

[23] J. Manzanares-Martínez, F. Ramos-Mendieta, and P. Halevi, Proc. SPIE, **5511**, 191 (2004).

[24] J. Manzanares-Martínez, F. Ramos-Mendieta, and P. Halevi, Appl. Phys. Lett., **87**, 101110 (2005).

[25] D. G. Gevaux, A. J. Bennett, R. M. Stevenson et al, Appl. Phys. Lett. **88**, 131101 (2006).

[26] P. Halevi, A. S. Sánchez, and E. Galindo-Linares, Opt. Commun., **269**, 351 (2007).

[27] S. W. Leonard, H. M. van Driel, J. Schilling et al, Phys. Rev. B **66**, 161102 (2002).

[28] H. W. Tan, H. M. van Driel, S. L. Schweitzer et al, Phys. Rev. B **72**, 165115 (2005); F. Raineri, C. Cojocaru, R. Raj et al, Opt. Lett. **30**, 64 (2005).

[29] J. P. Mondia, H. W. Tan, S. Linder et al, J. Opt. Soc. Am. B, **22**, 2480 (2005); A. D. Bristow, D. O. Kundys, A. Z. García-Déniz et al, Opt. Lett. **31**, 2284 (2006).

[30] S. F. Preble, W. R. Almeida, and M. Lipson, Proc. SPIE, **5511**, 10 (2004).

[31] A. Irce, G. Breglio, and A. Cutolo, A. Electron. Lett., **39**, 232 (2003).

[32] A. Liu, R. Jones, L. Liao et al, Nature, **427**, 615 (2004).

[33] E. M. Purcell, Phys. Rev. **69**, 681 (1946).

[34] E. Snoeks, A. Lagendijk, and A. Polman, Phys. Rev. Lett. **74**, 2459 (1995).

[35] S. V. Gaponenko V. N. Bogomolov, E. P. Petrov et al, J. Lightw. Tech **17**, 2128 (1999).

[36] A. Irrera et al, in *Towards the First Silicon Laser*, eds. L. Pavesi et al, Kluwer(2003) p. 29.

[37] P. Y. Yu and M. Cardona, *Fundamentals of Semiconductors*, 2nd. ed., Springer (1999) p. 340.

[38] J. Manzanares-Martínez, F. Ramos-Mendieta, and P. Halevi, Appl. Phys. Lett. **87**, 101110 (2005).

[39] E. Galindo-Linares, P. Halevi, and A. S. Sánchez, unpublished.

[40] Ling Liao et al, IEEE J. Quant. Elect. **41**, 250 (2005).

[41] H. S. Kitzerow, and J. P. Reithaimer, in *Photonic Crystals: Advances in Design, Fabrication, and Characterization*, eds. K. Busch et al, Wiley (2004), p. 174.

[42] K. Busch and S. John, Phys. Rev. Lett. **83**, 967 (1999); D. Kang et al, *ibid.* **86**, 4052 (2001);

[43] E. Yablonovitch, Phys. Rev. Lett. **62**, 1742 (1989).

[44] *Handbook of Optics*, Vol. 1, 2nd. ed., M. Bass, Editor in Chief, Mc Graw-Hill,p. 11.29.

[45] J. D. Joannopoulos, R. D. Meade, and J. N. Winn, *Photonic Crystals*, Princeton (1995);K. Sakoda, *Optical Properties of Photonic Crystals*, Spinger (2001); S. Noda and T. Baba, eds. *Roadmap on Photonic Crystals*, Kluwer (2003).

[46] Just such a PC was studied by M. Patrini et al, J. Appl. Phys. **92**, 1816 (2002).

[47] J. P. McKelvey, *Solid State and Semiconductor Physics*, Harper and Row (1966).

[48] J. D. Wiley, in *Semiconductors and Semimetals*, eds. R. K. Williardson and A. C. Beer (1975), vol. 10; R. A. Smith, *Semiconductors* (Cambridge, 1978).

[49] R. S. Muller and T. I. Kamins, *Device Electronics for Integrated Circuits* Wiley, (1986), 2nd ed.

[50] R. J. Glauber and M. Lewenstein, Phys. Rev. A **43**, 467 (1991).

[51] P. Halevi and A. S. Sánchez, Optics Comm. **251**, 109 (2005).

Publications and Congresses

- E.Galindo-Linares, P. Halevi, and A. S. Sánchez, "Tuning of one-dimensional Si/SiO$_2$ photonic crystals at the wavelength of 1.54μm", submitted to APL.

- P. Halevi, A. S. Sánchez and E. Galindo-Linares; "Tuning Si/SiO$_2$ 1.54μm", Opt. Commun., **269**, 351 (2007).

- E. Galindo-Linares, Adán S. Sánchez and P. Halevi "Tuning of the spontaneous emission in a one-dimensional photonic crystal", American Physical Society March Meeting 2005. Baltimore, USA; March 16-20, 2006.

- E. Galindo Linares, Adán S. Sánchez and P. Halevi "Sintonización de cristales fotónicos uni-dimensionales a 1.54μm", INAOE, Séptimo encuentro de investigación. Tonantzintla, Puebla, México; 8 y 9 de Noviembre, 2006.

- E. Galindo Linares, Adán S. Sánchez and P. Halevi "Sintonización de la respuesta óptica de un cristal fotónico unidimensional en una longitud de onda de comunicaciones", Sociedad Mexicana de Física, XLIX Congreso Nacional de Física. San Luis Potos, México; 16-20 de Octubre, 2006.

- Elizabeth Galindo, Adán S. Sánchez and P. Halevi "Tuning of the spontaneous emission in a one-dimensional photonic crystal", American Physical Society March Meeting 2005. Los Angeles, CA, USA; March 21-25, 2005.

- E. Galindo Linares, A. Sánchez Sánchez and P. Halevi "Sintonización de la emisión espontánea en un cristal fotónico unidimensional", Sociedad Mexicana de Física, XLVII Congreso Nacional de Física. Hermosillo, Sonora, México; 25-29 de Octubre, 2004.

Tuning of one-dimensional Si/SiO$_2$ photonic crystals at the wavelength of $1.54\mu m$

E. Galindo-Linares and P. Halevi
Instituto Nacional de Astrofísica, Óptica y Electrónica
Apdo. Postal 51, Puebla, Pue. 72000, México

Adán S. Sánchez
Intel Mexico Research Center, Guadalajara 45600, México.

We simulate the tuning of reflectance of a one-dimensional photonic crystal (PC) by means of charge injection. The PC is constituted from highly doped silicon layers alternating with silicon oxide layers. The wavelength of the light is assumed to be the important communications wavelength of $1.54\mu m$. A realistic simulation shows that sensitive tuning, and switching as well, can be achieved for an impurity density $\sim 10^{19}/cm^3$ even for superlattices only a few periods long. The reflectance results are satisfactorily interpreted in terms of photonic band structure calculations.

Photonic Crystals (PCs) by now constitute a mature field, with numerous applications. One of these is *tuning*, namely the optical response of the PC is altered by means of some external agent. Such control of the response −for instance reflectance or spontaneous emission− includes the special case of *switching* it on and off. The large number of papers published on the subject of tuning of PCs may be classified as follows. 1) Producing *structural changes* in the PC, without changing the material properties of the ingredients[1]. This has been achieved by miscellaneous methods such as mechanical stress, a piezoelectric material subject to an electric field, insertion of diodes, and the tip of an atomic force microscope. 2)A second way of control is obtained by the incorporation of a *ferroelectric or a ferromagnetic substance* within the PC; an applied electric or magnetic field, respectively, will then alter the photonic band structure and, consequently, the response.[2] 3) Further, two papers exploit the *thermo-optic effect* to tune wave propagation in PC waveguides and channel-drop devices.[3] 4) Infiltration of the PC with a *liquid crystal* −remarkably sensitive to temperature changes, pressure, and applied electric or magnetic fields− is a much favoured approach.[4] 5) In continuation, illumination by an *intense laser beam* can produce small (non-linear) changes in the refractive index of a constitutive material of the PC. Here advantage is taken of the electro-optic or the photorefractive effects in order to tune diverse PC structures.[5] 6)The last category of tuning considered −and the one that concerns us in this Letter− is based on the creation of *electron-hole pairs* in a semiconducting constituent of the PC. This can be accomplished either by heating the semiconductor (T-tuning) or by charge injection (N-tuning).[6–17]

T-tuning is most effective for narrow-gap semiconductors, such as InSb, that give rise to large densities of free electrons − excited thermally from the valence band to the conduction band. This was shown to lead to dramatic changes in the photonic band structure of InSb cylinders in a square lattice.[6] Similar results were obtained in Ref. 7, and the possibility of controlling the direction of wave propagation in a Y-shaped, two-dimensional (2D) PC waveguide was proposed.[8] Recently, simulations of T-tuning in 1D[9] and 2D[10] PCs were also performed. And, the tuning of pulses traversing 1D and 2D PCs with defects was reported in Refs. 11 and 12, respectively. Moreover, T-tuning of InAs quantum dots in a PC cavity can enhance or suppress their rate of spontaneous emission.[13]

As for N-tuning, the charge injection may be realized either by means of optical excitation or by forward biasing a p-n junction. The latter technique is based on free carrier injection into the intrinsic region of a forward biased p-i-n device.[18] Faster carrier density changes are achieved by embedding a metal-oxide-semiconductor structure in optical devices.[19] Theoretical investigations, mostly on strongly doped n-Si PCs were carried out for 2D photonic band structure[6], for simulation of CW transmission in 1D[9] and 2D[10] PCs and for transmission of pulses in 1D[11] and 2D[12] PCs with defects. Recently it was also shown that the rate of spontaneous emission of an atom (modeled by a dipole), embedded in a superlattice, can be substantially altered by N-tuning.[14] On the experimental side, optical excitation was prefered, achieving ultrafast tuning in 2D PCs.[15] Guided modes in PC waveguides were also tuned[16] and it was demonstrated that a nanocavity in a PC can be optically controlled.[17]

In this Letter we show that sensitive N-tuning can be achieved in a simple configuration, with technologically important and readily processable materials, and at an important infrared wavelength. The configuration is a 1D PC or superlattice; the materials are silicon and silicon oxide, and the wavelength is $1.54\mu m$ − widely employed in optical communications (relying on Er-doped optical fiber amplifiers). We have already demonstrated that tuning of the spontaneous emission is feasible for just such a system at the same wavelength.[14]

In what follows we simulate reflectance measurements, for a n-Si/SiO$_2$ superlattice, as function of the donor impurity concentration in the Si layers. This concentration, N, is our tuning agent and it is assumed to be high, $N \sim 10^{19}/cm^3$ − which is necessary for achieving sensitive tuning with the wavelength fixed at $\lambda_0 = 1.54\mu m$.

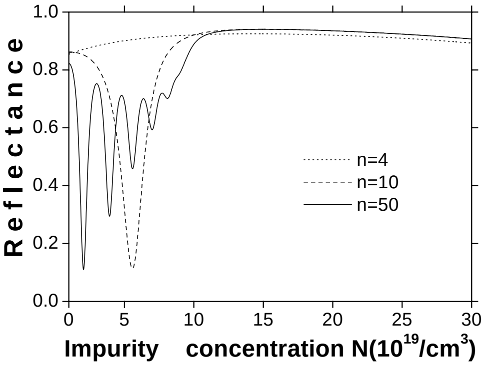

FIG. 1: Reflectance for a one-dimensional photonic crystal of Si and SiO_2 layers. The silicon layers are strongly doped and we show how the reflectance is tuned by varying the impurity concentration. Four, 10, and 50 periods in the length of the superlattice are considered. The period is $d = 0.73 \mu m$.

Although such high concentrations could be expected to be destructive for a device based on these ideas, we will demonstrate that a judicious choice of the parameters can minimize undesirable absorption. We use the plasma model for a realistic description of the n-Si dielectric constant:

$$\frac{\epsilon(\omega)}{\epsilon_\infty} = 1 - \frac{\omega_{pe}^2}{\omega(\omega + i/\tau_e)} - \frac{\omega_{ph}^2}{\omega(\omega + i/\tau_h)}. \quad (1)$$

Here, ϵ_∞ is the high-frequency dielectric constant, $\tau_{e,h}$ are the electron and hole scattering times, and $\omega_{pe,h} = (4\pi n_{e,h}^2 e^2 / m_{e,h} \epsilon_\infty)^{1/2}$ are their plasma frequencies. The densities of the electrons n_e in the conduction band and of the (effective)holes n_h in the valence band are related to the impurity concentration N by $n_{e,h} = (n_i^2 + N^2/4)^{1/2} \pm N/2$. Because the intrinsic concentration n_i is very small in comparison to N, actually $n_e \simeq N$ and $n_h \simeq n_i^2/N$. See Ref. 9 for the numerical values of the parameters.

Usually, the period of the superlattice d is chosen to be comparable to the operational wavelength λ_0. If we take $d = 0.73 \mu m$, with the Si layers occupying a fraction $f = 0.5$, Fig. 1 is obtained for the reflectance. Note that, for $n = 50$ periods, the $R(N)$ curve is initially very steep, with a 70% decrease of the reflectance, which surely is a desirable tuning characteristic. Moreover, if we eliminate the absorption (by substituting $\tau_{e,h} = \infty$ in eq.(1)) the resulting figure is indistinguishable on this scale. On the downside, however, the response is qualitatively dependent on the number of periods. This aspect can be remedied by selecting a much larger period, $d = 7 \mu m$, Fig. 2. A steep response is seen for $N \simeq 5 \times 10^{19}/cm^3$, which is not much sensitive to either the number of periods or to absorption (bottom panel; in the top panel absorption has been "turned off"). By changing N from 4.14 to $5.74 \times 10^{19}/cm^3$, *switching* is also possible, for the reflectance drops from a high value (0.8 for $n = 10$) to zero.

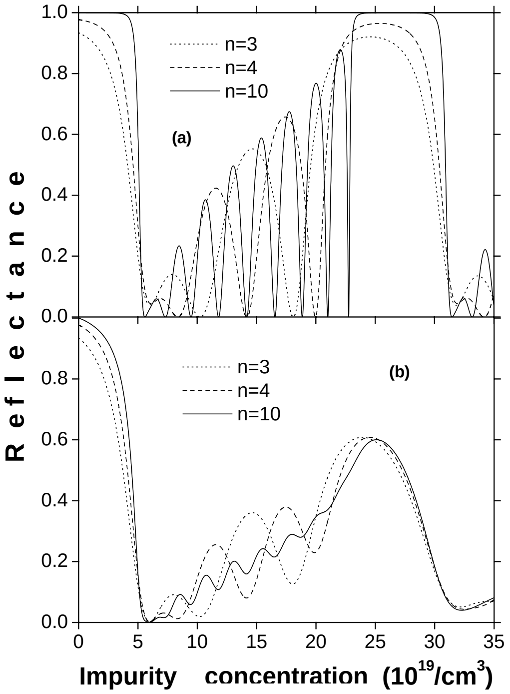

FIG. 2: As in Fig. 1 for a period $d = 7 \mu m$, now considering superlattices three, four, and 10 periods long. Absorption has been turned off in (a) and turned on in (b). Note that the band edge at $N \simeq 5 \times 10^{19}/cm^3$ is appropriate for tuning.

For greater values of the concentration, though, the reflectance is strongly impacted by dissipation, so that the regime $N > 6 \times 10^{19}/cm^3$ is unsuitable for tuning.

The three almost vertical lines in Fig. 2(a), at $N \simeq 5$, 23 and $31 \times 10^{19}/cm^3$, have the appearance of band edges that are characteristic of $R(\omega)$ plots. To convince ourselves that they are, indeed, band edges −although in the $R(N)$ representation (with ω as a parameter)− let us look at two different renditions of the photonic band structure in Fig. 3. Here, for the unlimited PC, the frequency ω is plotted as function of the Bloch wave vector k (N being a parameter) in part (a) and as function of the impurity density N (now with k as the parameter) in part (b). The heavy horizontal line represents the frequency $\omega_0 = 2\pi c/\lambda_0$. As Fig. 3(a) clearly shows, this line lies completely in the band gap for $N \lesssim 3 \times 10^{19}/cm^3$ − between the curves "3" above and below the ω_0 line. For this reason, in this range of N the light must be completely reflected in the ideal, absorptionless and infinite superlattice − as is suggested by Fig. 2(a). For $N = 5 \times 10^{19}/cm^3$ the lower curve "5" already intersects the ω_0 line, thus making optical modes available for propagation. Fig. 3(b) confirms this reasoning and, moreover, the left edge ($k = \pi/d$) of the central band crosses the line ω_0 at the precise value of the transition from the low-N stop band to a pass-band − at $N = 4.9 \times 10^{19}/cm^3$. For greater N values Fabry-Perot oscillations of the re-

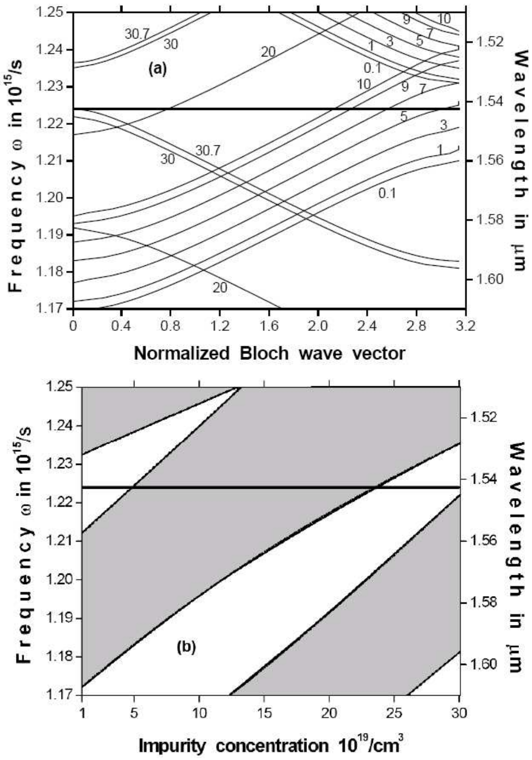

FIG. 3: Band structure for the (infinite) photonic crystal considered in Fig. 2(a). The frequency (wavelength) is plotted on the left (right) side axis as function of the normalized Bloch vector kd (with N as parameter) in part (a) and *vice versa* in part (b). In (a), the numbers next to each line are the values of N in $10^{19}/cm^3$. The horizontal lines mark the frequency corresponding to the wavelength of $1.54\mu m$.

flectance are apparent in Fig. 2(a) and, in a damped form, also in Fig. 2(b). Entirely similar considerations are applicable to the band edge at $N \simeq 31\times 10^{19}/cm^3$ in Fig. 2(a). And a glance at the lower curve "30.7" in Fig. 3(a) reveals that it is just tangent to the ω_0 line – which fixes the band edge at $30.7 \times 10^{19}/cm^3$. As for the band edge at $N \simeq 23\times 10^{19}/cm^3$ in Fig. 2(a), we note that in Fig. 3(a) the curve "20" crosses the ω_0 line, while this line lies between the curves "30", namely in a band gap. The precise position of the band edge is given by the intersect, in Fig. 3(b), of the right side edge of the central band (for $k = 0$) with the ω_0 line – $N = 23.6\times 10^{19}/cm^3$.

Why is the first stop-band, at $N \lesssim 5\times 10^{19}/cm^3$, quite insensitive to absorption, while the second stop-band, centered at about $27 \times 10^{19}/cm^3$, suffers strong attenuation? This is readily explained by the fact that, as N increases, so does the scattering of the free electrons from the impurities. Mathematically, this scattering manifests itself in smaller collision times $\tau_{e,h}$ in eq. (1).

We have thus shown that both tuning and switching of the reflectance is possible in a Si/SiO$_2$ one-dimensional photonic crystal at the technologically important wavelength of $1.54\mu m$. This could be accomplished by either optical or electrical charge injection, varying the impurity density at $N \sim 10^{19}/cm^3$, even with a small number of PC periods. In the case of electrical tuning a unit cell of four Si layers −p-type, intrinsic, n-type, and oxide− could be advantageous. The first three layers would form a p-i-n diode and would serve to modify the carrier concentration, while the oxide layer would increase the dielectric contrast. Such tuning of the reflectance in photonic crystals could have a positive impact on silicon optical devices such as waveguides, modulators, and laser cavities.

---

[1] S. Iwamoto, S. Ishida, Y. Arakawa et al, Appl. Phys. Lett. **88**, 011104 (2006); I. Märki, M. Salt, and H. P. Herzig, Opt. Exp. **14**, 2969 (2006) and references therein.
[2] J. Zhou, C. Q. Sun, K. Pita et al, Appl. Phys. Lett. **78**, 661 (2001) and references therein.
[3] Y. A. Vlasov, M. O'Boyle, H. F. Hamann et al, Nature **438**, 65 (2005); T. Asano, W. Kunishi, M. Nakamura et al, *Elect. Lett.* **41**, 37 (2005).
[4] D. McPhail, M. Straub, and M. Gu, Appl. Phys. Lett. **86**, 051103 (2005) and **87**, 091117 (2005); P. Halevi, J. A. Reyes-Avendaño, and J. A. Reyes-Cervantes, Phys. Rev. E **73**, R040701 (2006) and references therein.
[5] A. Haché, and M. Bourgeois, Appl. Phys. Lett. **77**, 4089 (2000); Y. Yi, P. Bermel, K. Wada et al, Appl. Phys. Lett. **81**, 4112 (2002) and references therein.
[6] P. Halevi and F. Ramos-Mendieta, Phys. Rev. Lett. **85**, 1875 (2000).
[7] C. S. Kee and H. Lim, Phys. Rev. B. **64**, 121103 (2001).
[8] H. Takeda and K. Yoshino, Opt. Comm. **219**, 177 (2003).
[9] A. S. Sánchez and P. Halevi, J. Appl. Phys. **94**, 797 (2003).
[10] J. Manzanares-Martínez, F. Ramos-Mendieta, and P. Halevi, Phys. Rev.B **72**, 035336 (2005).
[11] *ibid*, Proc. SPIE, **5511**, 191 (2004).
[12] *ibid*, Appl. Phys. Lett., **87**, 101110 (2005).
[13] D. G. Gevaux, A. J. Bennett, R. M. Stevenson et al, Appl. Phys. Lett. **88**, 131101 (2006).
[14] P. Halevi, A. S. Sánchez, and E. Galindo-Linares, Opt. Commun., accepted for publication.
[15] S. W. Leonard, H. M. van Driel, J. Schilling et al, Phys. Rev. B **66**, 161102 (2002); H. W. Tan, H. M. van Driel, S. L. Schweitzer et al, *ibid*, 165115 (2005); F. Raineri, C. Cojocaru, R. Raj et al, Opt. Lett. **30**, 64 (2005).
[16] J. P. Mondia, H. W. Tan, S. Linder et al, J. Opt. Soc. Am. B, **22**, 2480 (2005); A. D. Bristow, D. O. Kundys, A. Z. García-Déniz et al, Opt. Lett. **31**, 2284 (2006).
[17] S. F. Preble, W. R. Almeida, and M. Lipson, Proc. SPIE, **5511**, 10 (2004).
[18] A. Irce, G. Breglio, and A. Cutolo, A. Electron. Lett., **39**, 232 (2003).
[19] A. Liu, R. Jones, L. Liao et al, Nature, **427**, 615 (2004).

Available online at www.sciencedirect.com
ScienceDirect

Optics Communications 269 (2007) 351–355

OPTICS
COMMUNICATIONS

www.elsevier.com/locate/optcom

Tuning and switching of the spontaneous emission in one-dimensional photonic crystals

P. Halevi, Adán S. Sánchez *, E. Galindo-Linares

Instituto Nacional de Astrofísica, Óptica y Electrónica, Apdo. Postal 51, Puebla 72000, Mexico

Received 17 June 2006; received in revised form 8 August 2006; accepted 10 August 2006

Abstract

If the modal density available to an excited atom is varied on the time scale of its lifetime, then we can expect the natural process of spontaneous emission (SE) to become dynamically manipulable. We consider various experimental possibilities and focus on an atom embedded in a photonic crystal designed to have a band edge in the vicinity of the frequency of the emitted light. Specifically, we calculate the rate of SE by erbium ions (radiating at the wavelength 1.54 μm) implanted in a one-dimensional silicon/silica photonic crystal. The semiconductor layers are assumed to be strongly doped; by tuning the impurity density the free carrier concentration changes and the photonic bands shift. As a result, the SE rate exhibits significant dependency on the level of charge injection.

Is it possible to vary spontaneous emission SE *actively* in real time? The very idea seems to involve a contradiction of terms: "spontaneous" implies a process that is inherent to the emitting atom, independent of experimental conditions! Nevertheless, in a pioneering paper [1], Purcell pointed out that SE is altered if the radiated field is constrained to satisfy a set of boundary conditions. In other words, the lifetime of an excited atomic state changes if the atom is located in a material environment, rather then radiating in free space. The rate of SE can be inhibited (and even prohibited) or enhanced, depending on the modal density (or density of states). If now the external conditions are varied on the time-scale of the excited state's lifetime, then we can expect that the natural process of SE becomes manipulable in real time. Is this feasible?

Let us consider three types of emitters. (a) *Rare earth ions*. In Er^{3+} the transition $4I_{13/2} \rightarrow 4I_{15/2}$, involving f-shell electrons, gives rise to emission at the important communications wavelength $\lambda_0 = 1.54\ \mu m$. The radiative lifetime (with the ions implanted in glass) is [2] $\tau = 22$ ms. (b) *Nanoparticles (quantum dots)*. These are frequently II–VI or III–V semiconductor compounds such as CdSe; they have been implanted in opal-type photonic crystals (PCs) [3]. Also, silicon nanocrystals have been implanted in silica [4]. Such quantum dots emit in the visible or near infrared; the lifetimes vary over many orders of magnitudes and can be as long as ~10 ms. (c) *Recombination in semiconductors*. The radiative lifetime due to recombination of photo-excited electrons and holes varies widely among semiconductors and depends strongly on the impurity density. For instance, with a density of $10^{17}/cm^3$ of majority carriers, the minority carrier lifetime in Si, Ge, and GaP is on the order of a ms. For intrinsic Si and Ge it is, respectively, 4.6 h and 0.61 s [5]. Next, are the temporal scales of tuning compatible with these lifetimes?

To answer this question, we discuss four possibilites of tuning of the optical response. (A) *Manipulation of the free-carrier density in semiconductors*. The mechanisms of thermal excitation and doping in PCs have been explored in a series of papers [6,7]. In particular, we found that the transmission of light through a one-dimensional (1D) PC of alternating Si/SiO_2 layers can be sensitively tuned at the wavelength 1.54 μm, [7] mentioned in (a). The intensity of high photoexcitation applied to semiconductors can be modulated as rapidly as the laser beam can be pulsed

---

* Corresponding author. Present address: Intel, Systems Research Center Mexico, Periferico Sur 7980, Ed. 4E, Guadalajara 45600, Mexico. Tel.: +52 33 35406158; fax: +52 33 35406099.

E-mail address: adan.sanchez@intel.com (A.S. Sánchez).

0030-4018/$ - see front matter © 2006 Published by Elsevier B.V.
doi:10.1016/j.optcom.2006.08.010

(repetition rates $\lesssim 1$ ns). An even more rapid band-edge tuning, in a 2D silicon PC, was achieved by means of 0.3 ps pulses [8]. And the response time of forward biasing at heterojunctions is ~1 ns [9]. (B) *Tuning of liquid crystal-infilled PCs* is a very active field, recently reviewed in Ref. [10]. Such tuning may be performed by changing the temperature or by applying a variable electric field, or by shining on pulsating high-intensity light; the response time is on the order of 1 ms. We quote a few notable papers [11]. (C) *Employing the thermo-optic effect*. Very recently, Vlasov et al. [12] have taken advantage of this effect to tune, in real time, the group velocity of waves propagating in a PC waveguide. The time-scale of the tuning was 0.1 μs. (D) *Nonlinear modulation of the refractive index of an insulator*. To quote Yablonovitch [13], "ideally, in nonlinear optics, we regard the refractive index of a medium to be a time-variable function totally under the control of the experimentalist". With solid state, (mode locked) pulsed lasers it is possible to achieve repetition rates as small as ~1 ns with fs pulses [14].

As we see from the list (A)–(D), the *slowest* tuning agent considered varies on the time scale of 1 ms. Then, comparing with the lifetimes for SE in the examples (a)–(c), we note that the *quickest* emission occurs also in about 1 ms. Hence, we come to the conclusion that external intervention in the process of SE should be feasible. We expect the rate of emission to depend in an important way on the details of the tuning agent. To quantify this problem we assume that the radiating atom is embedded in a dielectric medium whose permittivity ϵ is being dynamically tuned by some unspecified mechanism. If the temporal dependence $\epsilon = \epsilon(t)$ is given – what is the corresponding rate of SE?

We are not aware of any measurement of the SE by an atom in a dynamically varying host medium. If $\epsilon = \epsilon(t)$, the nature of the normal modes in the medium will strongly depend on the specific form of the time dependence. As a result, the behavior of the SE should also change qualitatively. Even for slow temporal variation of the dielectric function, the adiabatic principle cannot be expected to be indicative of the real-time behavior of the SE rate. A theory of SE in a temporally varying medium is now being developed by the first author (PH). For the time being, we will not concern ourselves with SE in real time. Rather, we will focus on a specific example that demonstrates appreciable dependence of the SE rate on an external agent of tuning. PCs [15] are often characterized by sharp photonic band edges and are, therefore, singularly attractive choices for hosting the radiating atom. This is true because the PC can be designed so as to have one of its band edges approximately coincide with the frequency of emission. Then a modest variation of the tuning agent is expected to produce a sizeable change in the emission rate. Regarding the choices (a)–(c) and (A)–(D) discussed above, we select the (a)–(A) combination. Specifically, this Letter is concerned with the simulation of SE by Er^{3+} ions embedded in a 1D PC of alternating Si and SiO_2 layers [16]. These materials have been selected because of their ease of fabrication, technological importance, and large dielectric contrast. The Er ions are chosen because they emit at the near-infrared wavelength $\lambda_0 = 1.54$ μm, very important for communications by optical fibers. We assume that the Si layers are strongly doped with impurity donor atoms. The concentration of these impurities is varied externally – and this is the tuning agent commented on above. Presumably, the mechanism would be carrier injection – either photoexcitation or forward biasing; the specifics are of no consequence for the considerations that follow. For highly extrinsic Si, the density of free electrons in the conduction band is practically equal to the donor density. The tuning of these densities modulates the dielectric constant of the semiconductor and this, in turn, shifts the photonic band edges. We then conclude that the tuning of the charge injection modulates the density of states available to the radiating atom. This explains the idea behind tuning of the SE rate for the particular example considered.

The semiconductor layers of the PC are modeled as a plasma of free electrons in the conduction band and free holes in the valence bands. The density of these, as function of the donor density N (and no acceptors) is [17] $n_{\mathrm{e,h}} = [(N/2)^2 + n_i^2(T)]^{1/2} \pm N/2$ where the intrinsic density $n_i(T)$ is very small in comparison to N. The corresponding electron and hole plasma frequencies are $\omega_{\mathrm{pe,h}} = (4\pi n_{\mathrm{e,h}} e^2/\epsilon_\infty m_{\mathrm{e,h}})^{1/2}$. Here ϵ_∞ is the high-frequency dielectric constant equal to 11.7 for Si. We use $m_e = 0.26 m_0$, where m_0 is the true electron mass. Also, the conductivity effective mass for holes (m_{h}) can be obtained from the effective masses of the light (m_{lh}) and heavy (m_{hh}) holes: $m_{\mathrm{h}} = m_{\mathrm{hh}}(1 + r^{3/2})/(r + r^{3/2})$, where $m_{\mathrm{hh}} = 0.49 m_0$ and $r = m_{\mathrm{hh}}/m_{\mathrm{lh}}$ [18]. The plasma model for the dielectric function takes into account absorption:

$$\epsilon(\omega) = \epsilon_\infty\{1 - \omega_{\mathrm{pe}}^2/[\omega(\omega + i/\tau_{\mathrm{e}})] - \omega_{\mathrm{ph}}^2[\omega(\omega + i/\tau_{\mathrm{h}})]\}. \quad (1)$$

The scattering times τ_{e} and τ_{h} are gotten from the carrier mobilities: $\tau_{\mathrm{e,h}} = m_{\mathrm{e,h}}\mu_{\mathrm{e,h/e}}$ with $\mu_{\mathrm{e,h}}$ derived from empirical models that take into account phonon and impurity scattering [19]. In Fig. 1 we plot the real and imaginary parts of Eq. (1) as function of the donor concentration N. The circular frequency has been fixed at $\omega = \omega_0 = 1.224 \times 10^{15}$/s, corresponding to the emission wavelength of interest $\lambda_0 = 1.54$ μm. Re ϵ and Im ϵ change rapidly for $N \gtrsim 10^{19}/\mathrm{cm}^3$; while Re ϵ decreases, Im ϵ increases with N. We are thus confronted with opposing demands. On the one hand, it is desirable to have N large enough for the plasma frequency to reach values $\omega_{\mathrm{p}}(N) \lesssim \omega_0$ (see inset of Fig. 1) where the tunability is largest. On the other hand, we also wish to keep absorption in check. As a reasonable compromise, we limit the impurity density to the range $10^{19} \leqslant N \leqslant 10^{20}/\mathrm{cm}^3$ where, for the upper limit, Im $\epsilon \simeq 0.0046$ Re ϵ. Henceforth, we will take into account only the real part of $\epsilon(N)$. We note that similar models were used for tuning the band structure and reflectance in 1D and 2D PCs [6,7]. For effective Bragg diffraction the period d should be of the same order as the wavelength ($d \sim$

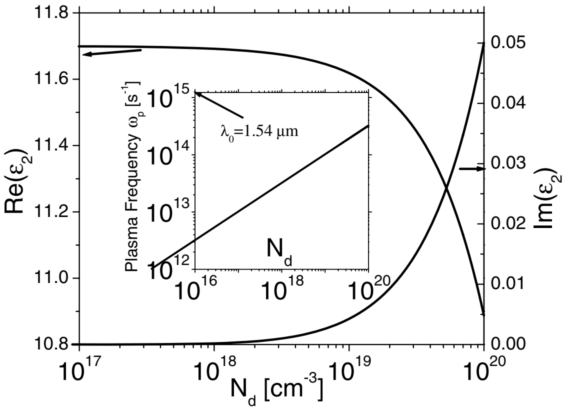

Fig. 1. Real (left axis) and imaginary (right axis) part of dielectric function of Si as function of impurity concentration. The wavelength is fixed at $\lambda_0 = 1.54\ \mu\text{m}$. The electron plasma frequency is shown in the inset. The arrow points at a hypothetical plasma frequency $2\pi c/\lambda_0$.

$\lambda_0 \sim \lambda_p = 2\pi c/\omega_p$). We have chosen $d = 0.73\ \mu\text{m}$ and layers of equal thickness. Using $\epsilon_1 = 2.09$ [18] for the silica layers and ϵ_2 given by the *real part* of Eq. (1) for the silicon layers, we obtain the band structure shown in Fig. 2. At low frequencies ($\omega \lesssim \omega_p$), a forbidden gap just below the first band appears in the band structure. Because the lower edge of the first band approximately coincides with ω_p, this gap is associated with the fact that for $\omega \lesssim \omega_p$, Re $\epsilon < 0$ and light cannot propagate in the semiconductor. The first band is the most sensitive to change in N because $\omega \sim \omega_p$. The PC considered was designed to give rise to an on-axis band edge around $\lambda = 1.54\ \mu\text{m}$, see the inset in Fig. 2. Thus, when $N = 10^{20}/\text{cm}^3$ the lower edge of the third band is just above $\omega_0 = 1.224 \times 10^{15}/\text{s}$ (corresponding to $\lambda_0 = 1.54\ \mu\text{m}$). For this frequency then, the *radiative* density of modes (with $k_\parallel < \omega/c$) vanishes and there can be no SE. On the other hand, if $N = 10^{19}/\text{cm}^3$, the frequency $\omega = 1.224 \times 10^{15}$ is located within the third allowed band and, consequently, the radiative density of modes is finite and radiation *can* occur. In Ref. [20] it was found that the SE changes abruptly at the on-axis band edges if the radiating atom is located at an antinode of the modes.

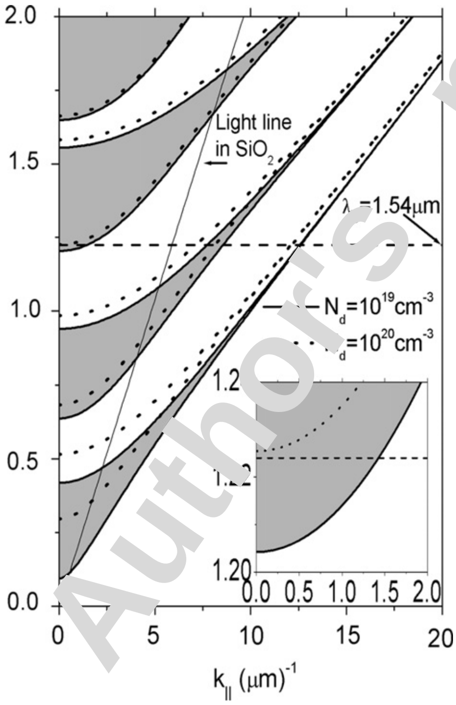

Fig. 2. TE band structure of a one-dimensional photonic crystal with period $d = 0.73\ \mu\text{m}$. Alternating Si and SiO_2 layers have equal widhts. Two values of the electron concentration are considered: $N = 10^{19}$ and $10^{20}/\text{cm}^3$. Gray areas correspond to allowed bands for the lower concentration. For the higher concentration, only the band edges are shown (dotted). In the inset, the lower band edges of the third band are amplified for both concentrations.

Now we proceed to calculate the rate of SE of an atom hosted by the above described PC. Glauber and Lewenstein [21] have developed a modal quantum electrodynamical theory for the SE rate of an atom embedded in an inhomogeneous dielectric medium, characterized by an arbitrary, position-dependent dielectric function $\epsilon(\mathbf{r})$. A similar, classical theory, was derived by Dowling and Bowden [22], who replaced the two-level atom by a dipole (moment $\boldsymbol{\mu}$) oscillating with the frequency $\omega_0 = (E_2 - E_1)/\hbar$. It is important to observe that the two theories [21,22] are equivalent because the Wigner–Weisskopff approximation, namely weak coupling of the emitted light to the atom, was assumed in Ref. [21]. This, in fact, corresponds to the situation observed in most experiments of SE. The main result of Dowling and Bowden [22] is the radiated power

$$P_p = \pi^2 \omega_0^2 \int d\mathbf{k} |\mathbf{a}_{\mathbf{k}p}(\mathbf{r_0}) \cdot \boldsymbol{\mu}|^2 \delta(\omega_{\mathbf{k}p} - \omega_0), \quad (2)$$

where the index p stands for TE or TM polarization, $\omega_{\mathbf{k}p}$ are the frequency eigenvalues, $\mathbf{a}_{\mathbf{k}p}(\mathbf{r_0})$ are the vector potential eigenvectors evaluated at the atom's position, the Dirac-delta function takes care of energy conservation, and the integration is over all normal modes for a given polarization. The SE rate is, simply, $\Gamma_p = P_p/\hbar\omega$.

Very recently, we have applied Eq. (2) to the calculation of the emission rate by an atom embedded in an (undoped) 1D PC [20,23]. Here we investigate the variation, with impurity concentration, of Γ_p for the Si/SiO_2 PC described above. In Fig. 3 we show the rate of emission as a function of the emitter's position for several carrier concentrations. The decay rate is normalized to the rate of emission in vacuum ($\Gamma/\Gamma_0 = P/P_0$). It is seen that the tunability is considerably greater for an ion embedded in the SiO_2 (white background), than it is for an ion in the Si (grey). For dipoles oriented parallel to the interfaces, the rate of emission into TE modes, Fig. 3(a), is very sensitive to N. When the donor concentration of Si is $10^{20}/\text{cm}^3$ there is no radiative mode because the lower edge of the third band is slightly above the frequency of the spontaneously emitted light. Thus, for this carrier concentration, the radiative contribution to the rate of emission vanishes for any position of the atom. Decreasing the carrier concentration, the rate of emission becomes finite when the lower edge of the third band shifts to frequencies that are below

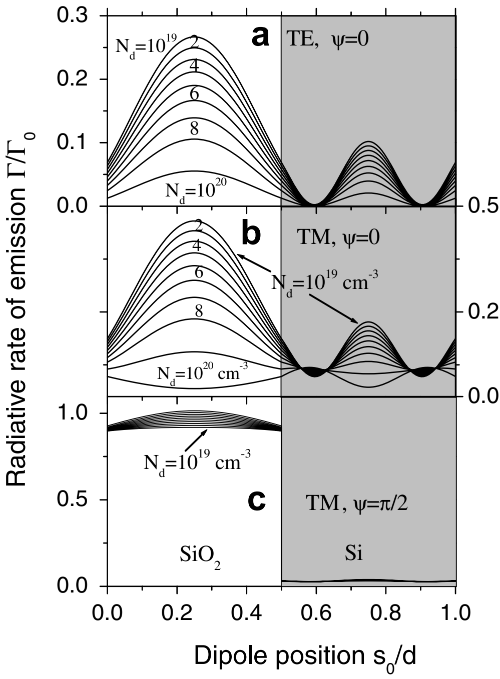

Fig. 3. Radiative contribution to the rate of spontaneous emission by an Er ion (at $\lambda = 1.54$ μm) implanted in a Si/SiO$_2$ one-dimensional photonic crystal. The rate of emission is normalized with that in air and is plotted as function of the donor impurity concentration and of the ion's position in the SiO$_2$ (left) and Si (right) layers. (a) TE modes, (b) TM modes for dipole parallel to the interfaces, and (c) TM modes for dipole perpendicular to the interfaces.

1.224×10^{15} s^{-1} (see the behavior of the on–axis band edge near $\lambda = 1.54$ μm in Fig. 2). This means that the emitted light can now couple to radiative modes. The emitter's position at which the rate of emission is most sensitive to changes in the carrier concentration is $s_0 = 0.25$ (at the middle of the SiO$_2$ layer). The antinodes of the electric-field at the lower band edges indeed coincide with the middle of the low-index layers, as found in Ref. [20]. If $\mathbf{p}$ forms an angle ψ with the interface, then Γ plotted in Fig. 3(a) must be multiplied by $\cos^2\psi$.

Consider an excited Er ion at the middle of a SiO$_2$ layer of a PC with $N = 10^{19}$/cm^3. It would radiate TE–polarized light at a rate $\Gamma \simeq 0.27\Gamma_0$. If, now, the carrier concentration is raised abruptly to 10^{20}/cm^3, the radiative TE–polarized emission will be prohibited. It is notable that this *switching* occurs when the dielectric function of Si suffers a change of only 6% (see Fig. 1). On the other hand, a *gradual* variation of the free-electron concentration from 10^{19} to 9×10^{19}/cm^3 would result in *tuning* of the SE. In contrast to the emission into radiative modes, the rate of emission into evanescent modes (not shown in Fig. 3) is much less sensitive to change in carrier concentration.

For TM polarization, two independent orientations (parallel and perpendicular to the interfaces) contribute to the SE. For dipoles parallel to the interfaces [$\psi = 0$, Fig. 3(b)], the radiative contribution to the SE presents considerable change when the carrier concentration varies from 10^{19} to 10^{20}/cm^3. The radiative rate of emission, however, never vanishes because the Brewster effect gives rise to closing of the band gaps for $0 < k_\parallel < \omega/c$. When the dipole is perpendicular to the interfaces [$\psi = \pi/2$, Fig. 3(c)], the coupling of the light to the dipole is quite weak; therefore, the rate of emission is not very sensitive to changes in the carrier concentration. Also, the total rate of emission is discontinuous across the interfaces. This is a result of the discontinuity of the component of the electric field normal to the interfaces.

The explicit dependence of the emission rate on the impurity density is displayed in Fig. 4. In part (a) the emitter is positioned in the middle of a silica layer. If the dipole moment is parallel to the interfaces, we observe considerable tunability for both polarizations, and the TE component strictly vanishes for $N \cong 9.4 \times 10^{19}$/cm^3. The discontinuity in the slope $d\Gamma/dN$ at this concentration persists even for a uniform distribution of the donors in the SiO$_2$ layer, Fig. 4(b). Here we averaged over all the dipole positions and orientations and over the two polarizations.

In this paper we have calculated the rate of SE of an atom embedded in a tunable 1D PC. We designed it so that it has a band edge near the frequency of the spontaneously emitted light corresponding to the important wavelength $\lambda = 1.54$ μm. Therefore, we obtain considerable sensitivity of the radiative SE on the donor impurity density, especially when the emitter's position coincides with an antinode of the normal modes. The results presented are a demonstration, through an example, of the idea that it should be possible to intervene *actively* in the process of SE. As discussed in this Letter, in principle there are many

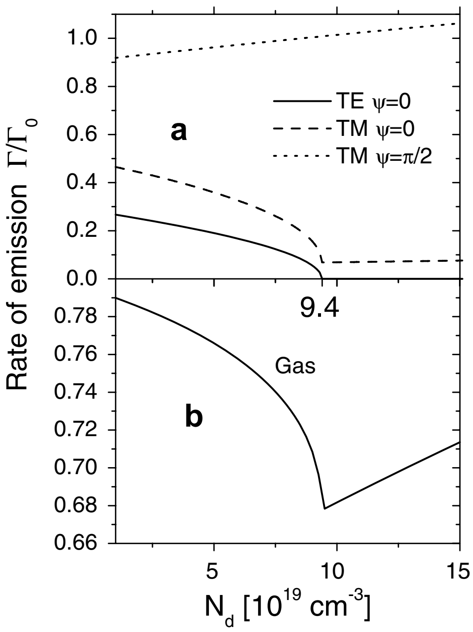

Fig. 4. Normalized rate of spontaneous emission by an Er ion as function of the impurity density in the layers. (a) The radiating ion is located at the center of SiO$_2$ the layer; note that for TE polarization $\Gamma = 0$ for $N \geqslant 9.4 \times 10^{19}$/cm^3. (b) Average rate of SE (per ion) for Er ions evenly distributed in the layer.

other possibilities for manipulating the relaxation of an atom via photon emission. We believe that dynamic alteration of SE is feasible experimentally. This could have important consequences for sources of light such as LEDs and lasers.

References

[1] E.M. Purcell, Phys. Rev. 69 (1946) 681.
[2] E. Snoeks, A. Lagendijk, A. Polman, Phys. Rev. Lett. 74 (1995) 2459.
[3] S.V. Gaponenko et al., J. Lightw. Tech. 17 (1999) 2128.
[4] A. Irrera et al., in: L. Pavesi et al. (Eds.), Towards the First Silicon Laser, Kluwer, 2003, p. 29.
[5] P.Y. Yu, M. Cardona, Fundamentals of Semiconductors, second ed., Springer, 1999, p. 340.
[6] P. Halevi, F. Ramos-Mendieta, Phys. Rev. Lett. 85 (2000) 1875;
C.S. Kee, H. Lim, Phys. Rev. B. 64 (2001) 121103;
H. Takeda, K. Yoshino, Optics Commun. 219 (2003) 177;
A.S. Sanchez, P. Halevi, J. Appl. Phys. (Commun.) 94 (2003) 797;
J. Manzanares-Martínez, F. Ramos-Mendieta, P. Halevi, Phys. Rev. B 72 (2005) 035336;
J. Manzanares-Martínez, F. Ramos-Mendieta, P. Halevi, Appl. Phys. Lett. 87 (2005) 101110.
[7] E. Galindo-Linares, P. Halevi, A.S. Sanchez, unpublished.
[8] S.W. Leonard et al., Phys. Rev. B 66 (2002) R161102.
[9] Ling Liao et al., IEEE J. Quant. Elect. 41 (2005) 250.
[10] H.S. Kitzerow, J.P. Reithaimer, in: K. Busch et al. (Eds.), Photonic Crystals: Advances in Design, Fabrication, and Characterization, Wiley, 2004, p. 174.
[11] K. Busch, S. John, Phys. Rev. Lett. 83 (1999) 967;
D. Kang et al., Phys. Rev. Lett. 86 (2001) 4052;
P. Halevi, J.A. Reyes-Avendaño, J.A. Reyes-Cervantes, Phys. Rev. E, 73 (2006) R040701.
[12] Y.A. Vlasov et al., Nature 438 (2005) 65.
[13] E. Yablonovitch, Phys. Rev. Lett. 62 (1989) 1742.
[14] M. Bass, (Editor in Chief), Handbook of Optics, vol. 1, second. ed., Mc Graw-Hill, p. 11.29.
[15] J.D. Joannopoulos, R.D. Meade, J.N. Winn, Photonic Crystals, Princeton, New Jersey, 1995;
K. Sakoda, Optical Properties of Photonic Crystals, Spinger, 2001;
S. Noda, T. Baba (Eds.), Roadmap on Photonic Crystals, Kluwer, 2003.
[16] Just such a PC was studied by M. Patrini et al., J. Appl. Phys. 92 (2002) 1816.
[17] J.P. McKelvey, Solid State and Semiconductor Physics, Harper and Row, 1966.
[18] J.D. Wiley, in: R.K. Williardson, A.C. Beer, (Eds.), Semiconductors and Semimetals, vol. 10, 1975; R.A. Smith, Semiconductors Cambridge, 1978.
[19] R.S. Muller, T.I. Kamins, Device Electronics for Integrated Circuits, second ed., Wiley, 1986.
[20] A.S. Sánchez, P. Halevi, Phys. Rev. E 72 (2005) 056609.
[21] R.J. Glauber, M. Lewenstein, Phys. Rev. A 43 (1991) 467.
[22] J.P. Dowling, C.M. Bowden, Phys. Rev. A 46 (1992) 612.
[23] P. Halevi, A.S. Sánchez, Opt. Commun. 251 (2005) 109.